DESIGN OF Yb^{3+} DOPED LASER FOR INDUSTRIAL APPLICATION

By

Moses Simpungwe

A Dissertation submitted to the University of Zambia in partial fulfillment of the requirement of the Degree of Masters of Engineering in Telecommunications Systems

THE UNIVERSITY OF ZAMBIA

LUSAKA

2021

COPYRIGHT DECLARATION

All rights reserved. No part of this work may be reproduced without prior written consent from the author or The University of Zambia.

DECLARATION

I, Moses Simpungwe, do declare that this work is my own and that the work of other persons utilized in this research has been duly acknowledged. This work presented here has not been previously presented at this or any other university for similar purposes.

Signed: …….

Date: …….....

Supervisor:

Full name: …….

Signature……. Date…….

CERTIFICATE OF APPROVAL

This document by _____ is approved as fulfilling the requirements for the award of the degree of Masters of Engineering in _____of the University of Zambia.

Examiners

Examiner 1: ……Signature:……Date: ……..

Examiner 2: …….Signature :……Date: ……..

Examiner 3: ……Signature:……Date: ……..

Chairperson ……Signature :……Date: ……..

ABSTRACT

The design and development of ytterbium-doped fibre lasers (YDFLs) operating around 1018nm laser wavelength and pumped around 976nm has advanced in technology since the first ytterbium laser was tested in 1988. The fiber lasers are used in various sectors such as communications, material processing, medical to mention but a few. Laser designers have the great objective of ensuring that the parameters such as pump power, active fibre cable and ion concentration are optimized for better quality laser output power. Further, the right choice of the output coupling between the Dichroic mirror (DM) and Fibre Bragg Grating (FBG) help eradicate the challenges faced in laser device design in terms of power output. Previous studies have reported use of diode lasers operating around 976nm as pump sources and lasing around 1018nm. There are, however, few reports on pump source use of 980nm on ytterbium doped laser fibre in the literature. This study therefore sought to contribute to improving on the power output of the YDFLs operating in continuous wave (CW) mode. In this modeling, a 980nm wavelength pump source with a lasing value at 1018nm wavelength and Dichroic couplers are deployed. In modeling the Yb^{3+} doped Laser, a quantitative approach was used. Linear differential equations were solved in order to determine the optimized values for the variables. Simulations using Computer software simulation -MATLAB were conducted. Power output of 59.64W was achieved against pump power of 68W, giving a slope efficiency of 87.71%. The operational characteristics of this Yb^{3+} doped fiber laser device in bidirectional pumping promises significant applications in radar, laser machining, free space communication and medical treatment. The results, further, show that the fiber cable length, the ion concentration and the choice of reflectivity on the OC and HR are critical when designing a fiber laser. Based on the results from the model, this study recommends that a study of the model be conducted experimentally to ascertain if the theoretical results will match with the experimental results.

Keywords*: ytterbium doped fiber laser, diode pumped lasers, ytterbium, Dichroic mirrors, fiber bragg gratings, wavelength, pumping*

DEDICATION

To my family and friends, my beloved wife and children who have always been there for me.

ACKNOWLEDGEMENTS

I would like to express my gratitude and appreciation to all those who supported me with my research work. A special thanks to my Supervisor Dr Charles Lubobya for the guidance and support he rendered to me during the entire period of my research. My interaction with him really gave me encouragement to go further in pursuing the good results of the research. I further extend my appreciation to Dr Sampa Nkonde, Dr Brilliant Habeenzu and the Telecommunications Specialists from University of Zambia for providing me with the information and material that formed the basis of my study.

Finally, I offer my profound gratitude to my wife Hildah and my children Niza, Moses, Alinaswe and Twiza for their patience and encouragement.

Moses Simpungwe

TABLE OF CONTENTS

Declaration ii

Certificate of approval form……..……...……..……iii

Abstract…….iv

Dedication..... v

Acknowledgements vi

Table of contents……..vii

List of Figures..... xi

List of Tables..... xiii

List of symbols…….....…….xiv

List of Abbreviations..... xv

CHAPTER ONE: BACKGROUND TO THE STUDY 1

1.0 Introduction 1

1.1 Background..... 2

1.1.2 Theoretical Model……4

1.1.3 Proposed model components……...4

1.2 Statement of the Problem 5

1.3 Aim of the Study…….…….…6

1.4 Study Objectives..... 6

1.5 Research Questions 6

1.6 Significance of the Study..... 6

1.7 Scope of the Study..... 7

1.8 Ethical Consideration…….…….…….7

1.9 Structure of the Dissertation..... 7

1.10 Summary..... 8

CHAPTER TWO: LITERATURE REVIEW 9

2.0 Introduction 9

2.1 Main Concepts 9

2.1.1 Laser Principles 9

2.1.2 Absorption 10

2.1.3 Spontaneous Emission 11

2.1.4 Stimulated Emission 11

2.1.5 The Laser Phenomenon 11

2.1.6 Population Inversion 12

2.1.7 Laser Cavity design 12

2.1.8 Pumping scheme 13

2.1.9 Propagation modes 15

2.2 Ytterbium Doped Fibers 16

2.2.1 Spectroscopic data for Yb^{3+} doped fibers 16

2.2.2 Energy Level structure 17

2.3 Laser Generation around 1018nm 18

2.3.1 Double Clad fibers 19

2.4 Development of 1018nm YDFLs 19

2.5 Related Works 20

2.6 Critique of the Literature 22

2.5 Summary 23

CHAPTER THREE: Yb^{3+} DOPED LASERS MODEL 24

3.0 Introduction 24

3.1 Absorption and Emission cross sections 24

3.2 Rate Equations 24

3.3 Pump power and Signal power Equations 26

3.4 Theory of Fiber Laser 27

3.5 Theory of Fiber Amplifier……29

3.6 Reference model……30

3.7 Summary..... 30

CHAPTER FOUR: RESEARCH METHODOLOGY 32

4.0 Introduction 32

4.1 Research Design 32

4.2 Simulation Tools 32

4.3 Simulation setup 33

4.4 Assumptions and Constraints 36

4.5 Summary..... 36

CHAPTER FIVE: RESULTS, ANALYSIS AND DISCUSSION..... 37

5.0 Introduction 37

5.1 Results 1-Comparison results for two models..... 37

5.1.1 Output Power with respect to input pump power 37

5.1.2 Output power with respect to Cable length 38

5.1.3 Output power with respect to wavelength……..41

5.1.4 Pump power with respect to active fiber cable length……...42

5.1.5 Output power with respect to Yb^{3+} ion concentration…..……..….43

5.1.6 Results -1 summary…….……45

5.2 Results-2 results for a new model pumping at 980nm 45

5.2.1 Output power with respect to input pump power 45

5.2.2 Output power with respect to cable length 47

5.2.3 Output power with respect to wavelength…….……49

5.2.4 Pump power with respect to active fiber cable length..... 50

5.2.5 Output power with respect to Yb^{3+} ion concentration..... 50

5.2.6 Results-2 summary…….51

5.3 Summary..... 52

CHAPTER SIX: CONCLUSIONS,RECOMMENDATIONS AND FUTURE WORKS 53
6.0 Introduction 53
6.1 Conclusions 53
6.2 Recommendations 54
6.3 Future Research 54
6.4 Summary 54
References 55
Appendices 61
Appendix A.1: CODE for two models-comparative CODE 61
Appendix A.2: CODE for reference model 64
Appendix A.3: CODE for pump wavelength at 980nm 66
Appendix A.4: CODE for ion variation at HR=100% and OC=30% 68
Appendix A.5: CODE for pump power of 68W @ 980nm wavelength 70
Appendix A.6: Journal Paper Publication 73

LIST OF FIGURES

Figure 1: The conceptual model of Yb^{3+} doped fiber laser..... 4

Figure 2:Depiction of lasing processes 10

Figure 2.1(a): Generic scheme of a Laser…..12

Figure 2.1(b): Scheme of a Fiber Laser with FBGs as mirrors.....13

Figure 2.2(a): Co- pumping ……..14

Figure 2.2(b): Counter- pumping ……14

Figure 2.2(c): Bidirectional- pumping ……15

Figure 2.3: Ground-state absorption spectrum, emission spectrum, and energy diagram of Yb^{3+} in Silica……..……..16

Figure 2.4: The Yb^{3+} energy level structure, consisting of lower manifold ($^2F_{7/2}$) and upper manifold ($^2F_{5/2}$) with respective stark levels……..…..17

Figure 2.5(a): Three level system……...……18

Figure 2.5(b): Two level system……....18

Figure 2.6: Schematic of double clad pumping scheme……....19

Figure 3: Schematic of Bidirectional pumped linear cavity fiber Laser 27

Figure 3.1: Experimental set up of the 1018nm YDFL pumped by 976nm LDs in Bidirectional pumping configuration.....30

Figure 5: Modeling results of laser output power vs. Input pump power.....37

Figure 5.1: Modeling results of Laser output power vs. active fiber cable length.....38

Figure 5.1.1(a): Modeling results of Laser output @ 976nm pump wavelength.....40

Figure 5.1.1(b): Modeling results of Laser output @ 980nm pump wavelength.....40

Figure 5.2: Modeling results of Laser output power vs. wavelength.....41

Figure 5.3: Pump power along the fiber cable 42

Figure 5.4: Modeling results of Laser output at Nt of 1e25, Nt of 1e26, Nt of 1e27

deploying HR of 99.5% and OC of 14.9%.....43

Figure 5.5: Modeling results of Laser output at Nt of 1e25, Nt of 1e26, Nt of 1e27 deploying HR of 100% and OC of 30%.....44

Figure 5.6: Input Pump power vs. Laser output power.....46

Figure 5.7:Modeling results of Laser output power pumped at 48W,68W and 88W.46

Figure 5.8: Active fiber Cable length vs. Laser output power.....47

Figure 5.9: Output power efficiency of Laser with varying active cable length.....48

Figure 5.10: Wavelength vs. output power @ 980nm pump wavelength.....49

Figure 5.11: Pump power along the active fiber cable.....50

Figure 5.12: Modeling results of Laser output at Nt of 1e26, Nt of 1e27, Nt of 1e28 deploying HR of 100% and OC of 30%.....50

LIST OF TABLES

Table 4: Modeling parameters for the reference model and a new model..... 34

Table 4.1: Modeling Parameters for a new model pumped at 68W..... 35

Table 5: Output power with respect to active fiber cable length 39

Table 5.1: Output power with respect to active fiber cable length 42

Table 5.2: Output power with respect to Yb^{3+} Concentration @ HR=99.5% and OC=14.9%..... 44

Table 5.3: Output power with respect to Yb^{3+} Concentration @ HR=100% and OC=30%..... 45

Table 5.4: Pump power vs. Laser output power 47

Table 5.5: Output power with respect to active fiber cable length 48

Table 5.6:Output power with respect to Yb^{3+} Concentration 51

LIST OF SYMBOLS

Nt	Concentration of Ytterbium ions
N_1	Normalized population of Ytterbium in the lower energy level
N_2	Normalized population of Ytterbium in the upper energy level
R_{12}	Pump excitation rate
R_{21}	Pump de-excitation rate
W_{12}	Signal absorption rate
W_{21}	Signal emission rate
A_{21}	Spontaneous emission rate
τ	Fluorescence life time of Yb^{3+} ions
h	Plank's constant
v_p	Pump transition frequency
v_s	Signal transition frequency
σ_{R12}	Pump absorption cross section
σ_{R21}	Pump emission cross section
σ_{W12}	Signal absorption cross section
σ_{W21}	Signal emission cross section
I_p	Pump intensity
I_s	Signal intensity
$\Gamma_{p(\lambda=980)}$	Overlap factor of pump mode field with doped area
$\Gamma_{s(\lambda=1018)}$	Overlap factor of signal mode field with doped area
σ_p	$\sigma_{R21}+\sigma_{R12}$
σ_s	$\sigma_{W21}+\sigma_{W12}$
L	Fiber length
Yb^{3+}	Ytterbium ion

LIST OF ABBREVIATIONS

YDFLs	Ytterbium doped fiber Lasers
DM	Dichroic Mirror
FBG	Fiber Bragg Grating
CW	Continuous Wave
OC	Output Coupler
HR	Highly Reflective
FLs	Fiber Lasers
RE	Rare Earth
ESA	Excited State Absorption
Yb	Ytterbium
ASE	Amplified Spontaneous Emission
NA	Numerical Aperture
erb	Erbium
EDFL	Erbium Doped Fiber Laser
DCFs	Double Clad Fibers

CHAPTER ONE

1.0 Introduction

The ever-increasing demand for high power devices and high-speed transmission of voice, data and video has made optical communications a preferred medium of transmitting information, leading to new work on high-speed optical devices design such as lasers. A laser is a device that emits light through a process of optical amplification based on the stimulated emission of electromagnetic radiation produced by the atoms due to changes in the energy states in the material. The atoms promoted to higher energy states emit laser in the form of light by the process known as “stimulated emission”. Laser is an acronym for "light amplification by stimulated emission of radiation” [1]. A laser is created when the electrons in atoms in special glasses, crystals, or gases absorb energy from an electrical current or another laser and become excited. The Lasing process is made possible by three main components: A gain medium which can support a population inversion, an external exciter to create the population inversion in the gain medium and an optical resonator or cavity to create a high radiation density.

Over the years, fiber lasers (FLs) have become increasing known in the field of scientific and commercial application, largely as a result of the outstanding characteristics they portray [2-4]. Fiber lasers are best known for their high average power and beam qualities compared to other types of lasers. The critical part of high power fiber laser module is the rare earth (RE) doped active fiber cable.

Since 1961, when the first fiber waveguide was proposed [5], the progress of fiber lasers in terms of application and output powers has seen a huge successful technological development. High average powers and excellent beam exhibited in fiber lasers are critical to many industrial applications [6]. Fibers can be used both as active media and waveguides in laser systems [7]. In the rare earth elements, Neodymium was the first element to be doped with silica in 1964 to produce the neodymium doped fiber laser [7]. This was followed by Erbium doped fiber laser in 1987[8]. In 1988, Ytterbium doped fiber laser was proposed and demonstrated [9]. The simple electronic structure of ytterbium brings about a number of advantages for use in fiber lasers compared to other rare earth materials. The YDFL has the potential to generate short pulses with peak power of 100 kW at 1000nm wavelength [10].

YDFLs have been shown to be an ideal choice for lasing and amplifying in the 1000 – 1200nm spectral region [11-13]. Yb^{3+} is an attractive laser dopant because of its high cross section of absorption, high concentration doping capability, low quantum defect and simple electronic structure.

YDFLs have over the years attracted huge interest in different fields due to their excellent characteristics. Some of which are: power conversion efficiency, power scaling, and broad emission bandwidth [14-17]. YDFLs operating at 1018nm wavelength are used mostly in tandem pumping for power amplifiers [18-19].

1.1 Background

Unlike the conventional solid state lasers counterparts, fiber lasers depicts numerous benefits notably enhanced conversion efficiency, high beam quality, high output power, high stability with temperature, etc. These features attracts many applications which include but not limited to radar, laser machining, free space communication and medical laser treatment. Ytterbium has simple energy level diagram which portrays merely a ground state, $^2F_{7/2,}$ and meta-stable state, $^2F_{5/2}$ separated by nearly 10,000 cm^{-1}. This huge gap between the two states reduces some of the drawbacks, such as excited state absorption phenomenon (ESA), associated with other rare earth doped-fibers. The presence of ESA in the Ytterbium doped fibers reduces the pump efficiency and concentration quenching through transfer of energy between the interior sub levels [20]. Ytterbium has wide-ranging absorption band which ranges from slightly under 850 nm to over 1070 nm due to the $^2F_{7/2} \rightarrow {}^2F_{5/2}$ transition [21].Depending on the host, the radiative lifetime for the meta-stable state, $^2F_{5/2}$ usually ranges between 700-1400 μs [22]. Ytterbium ion doped materials are used in high power solid lasers and fiber lasers. Ytterbium doped fiber Lasers have two peak absorption regions: The lower region at 915nm wavelength and the upper region at 976nm wavelength. To achieve high power efficiency, by taking advantage of the low quantum defect, almost all 1018nm YDFL employ pump sources around 976nm wavelength.

Quantum defect is defined as the difference of photon energies between the pump and laser photons which set a lower limit to the loss in the conversion from pump power to laser power that sets an upper limit to the output power or optical-to-optical efficiency [23]. A small quantum defect between the pump and signal wavelength of

YB3+ leads to high efficiency exceeding 80% and this drastically reduces heat generation [24].

However, at 976nm pump wavelength, a challenge arises on how to stabilize the wavelength as chances of wavelength shifting are very high. This challenge is overcome by employing wavelength stabilized diode lasers. The wavelength shift can also be controlled by use fiber Bragg grating [20].YDFLs with relatively good power efficiencies have been reported in some previous studies [18-19].

Unlike other rare earth elements such as erbium, thulium, neodymium etc which are equally used as dopants in fiber lasers, Ytterbium ion does not have higher energy levels which significantly minimize the occurrence of multi-photon relaxation as well as excited state absorption (ESA). Ytterbium ions also have emission as well as absorption cross sections that are usually many times greater compared to other rare-earth ions in multi-component glasses. However, ytterbium doped silica glasses at 1018nm lasing have a serious gain competition around 1030nm.This is so because the local emission of Yb ions is around 1030nm.This competition brings about parasitic lasing [18]. There are a lot of theoretical models of the YDFL based on rate equations and power differential transitions with fixed or variant parameters of the fiber laser. The numerical analyses of pump power, fiber length and ion concentration and its effects on the YDFL have been studied in this model.

In this study, a theoretical model in continuous wave (CW) pumping mode is designed. Simulation is done by use of Matlab software. The effect of pump power on the ytterbium ion distribution between the upper and lower energy levels within a manifold is considered. Due to the huge gap between the ground state and the excited state, based on the energy level diagram, the redistribution of the ions between the two states is not considered. The study considered the standard rate equations for the two level system in describing the gain, and pumps and signal propagation characteristics of the active fiber. An extensive analysis was done, regarding the set of coupled propagation rate equations, without considering the effect of ESA and of amplified spontaneous emission (ASE) parasitic noises. The main difference of pumping at 976nm and 980nm wavelengths has been investigated in order to find the corresponding gain in terms of laser output power.

1.1.2 Theoretical Model

The conceptual model for the designed device involving Yb^{3+} doped fiber with 60 W output power is as outlined in Figure 1 below. The Dichroic coupler handles either 980 nm/1000 nm combination of wavelengths to efficiently couple both the -30 dBm input signal and 68W pump power. Pumping at 976nm wavelength is the peak of the ytterbium absorption spectrum, but the waveband of this peak is too narrow to use with confidence. Additionally, at 976nm pumping a fraction of the Yb ion is strongly quenched resulting into strong unbleachable absorption and loss of lasing [22]. This study, therefore, decided to use 980nm pumping to avoid the challenges mentioned above and also to achieve better slope efficiency. At 980nm pump wavelength, it is assumed that there is no ESA and ASE and therefore quenching is neglected and so is the fiber losses. Further, this theoretical model takes note that the pump at 980nm is a monochromatic signal. It also takes note that only one fundamental transverse mode is considered and neglects the higher order transverse modes of the laser cavity.

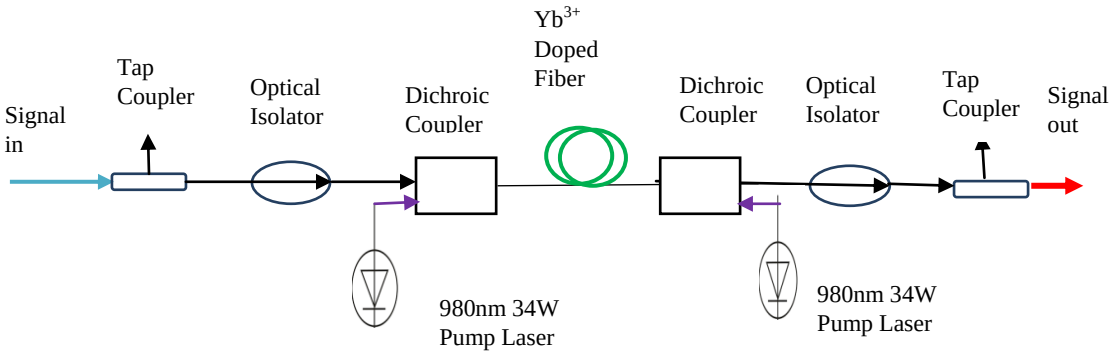

Figure 1: The conceptual model of Yb^{3+} doped fiber Laser device

1.1.3. Proposed model components

The model in figure 1 above deploys an active fiber cable whose purpose is to intensify a small optical beam, which propagates inside the cavity. In which case, the amplifier is "seeded" with a low power laser beam. The pumping scheme used is bidirectional.

Considering figure 1 above, Yb^{3+} Doped Fiber is an active fiber cable doped with ytterbium element. Ytterbium is a rare earth material used in doping silica glass to improve the characteristics of the active fiber cable such as low noise and gain in the output power. Coiling the gain fiber of an amplifier is one method utilized to effectively depress high-order modes [25].

The Tap coupler is used for tapping of signal to a particular direction in the Network. Connected to the Tap coupler is the Optical Isolator used to prevent the signal from moving in the opposite direction thereby reducing interference in the system. They are placed at the input and output ends to protect the seed and pump sources from back-reflections.

The Dichroic couplers are suitable for two wavelength input unlike the Fiber Bragg Grating which is suitable for multimode input and out wavelengths. Two pumps are used in this model. The Co-pump and the Counter pump both at 980nm wavelength. Co-pump gives better noise performance in the system. It has the characteristics of reducing noise in the system where as Counter pumping allows higher gains and therefore it is best suited for amplification in the system.

The system where the co-pump and counter pump are used at the same time is called Bidirectional pumping. Bidirectional pumping is applied to achieve a low noise and high power efficiency system. In this model, a theoretical Yb^{3+} doped fiber Laser device for industrial application is presented. The model is pumped at 980nm wavelength and lasing at 1018nm wavelength. The effects of fluctuations in the pump power, variations in the active fiber length and effects of variations of the active ion (Yb^{3+}) concentrations are extensively explored.

1.2 Statement of the problem

The doping of fiber with rare earth materials, such as ytterbium, to fabricate laser fibers has found great use in industrial applications [10].

In the last decade, ytterbium has been used as a sensitizer to Erbium [26] to fabricate fiber lasers and operate in the 1500nm range. However, it has been observed that when used as a dopant it produces high output power [27] but has limitations in the variations of the pump power, Yb^{3+} ions concentrations and active fiber length determination to an extent of: using a lot of pump power for little power output [26], using of less doped Yb^{3+} ions affecting the system performance [27-28] and failing to reach a suitable compromise between the active fiber length and system efficiency

[29]. Following intensive literature review on the currently used Ytterbium doped Fiber Lasers: it has been observed that too much pump power is used for production of little output power. Low Yb^{3+} ion concentrations levels produces low output power and difficulties in determining active fiber length leading to low efficiency in laser performance. This study proposed design of Yb^{3+} doped Fiber laser of 34W pump power in bidirectional mode. The pump and laser wavelength are 980nm and 1018nm respectively. The highly reflective (HR) and output coupler (OC) are in the Dichroic coupler as opposed to using Fiber Bragg Grating.

1.3 Aim of the study

The aim of the study was to theoretically design a Yb^{3+} doped laser to be used for industrial application such as Radar, Laser machining, free space communication, medical laser treatment etc. The device will have bidirectional pumping at 980nm pump source to reduce on noise, achieve more power output at lasing wavelength of 1018nm and have short active fiber cable.

1.4 Study Objectives

The main objective of the study was to design Yb^{3+} doped Fiber laser for industrial application and the specific objectives were:

To achieve optimal output power by varying the pump power, to achieve optimal output power by varying the active fiber length and to obtain Optimal output power by varying the doping levels in the Yb^{3+} ions.

1.5 Research questions

The research was guided by the following research questions:

How is high output power in Yb^{3+} doped Fiber Lasers in relation to pump power achieved?, how is high output power in Yb^{3+} Fiber lasers in relation to active fiber cable length achieved?, how is high output power in relation to Yb^{3+} ion concentration obtained?.

1.6 Significance of the study

The significance of the study is that once a good Yb^{3+} doped fiber laser is designed by using Yb^{3+}, it will reduce the cost of operations in industry because the amplification of the seemingly weak signal from the source will be pumped by having a good laser beam from the doped laser which can travel a long distance thereby reducing the number of amplifiers in the network and bringing efficiency in free space communication. This will also motivate the construction of the Yb^{3+}

doped Laser devices at cheap cost since the cable length will be short. It will also improve operations in laser machining and also in medical laser treatment.

1.7 Scope of the study

The scope of the study is to design the Yb^{3+} doped laser device for industrial application.

1.8 Ethical considerations

Telecommunication companies in Zambia such as Zamtel, Liquid Telecomms and Zesco have deployed fiber cable in providing telecommunications services. Ethical clearance was obtained from the University of Zambia Ethics Committee in anticipation of visiting these companies. It was later realized that there was no need for the visitation.

1.9 Structure of the Dissertation

The research report is divided into six chapters as outlined below.

Chapter One	Background to the Study: This chapter gave an overview of the study and its background. It covered the problem statement, research questions, objectives, scope and the significance of the study.
Chapter Two	Literature Review: This chapter contextualized the research by looking at the earlier studies regarding deployment of rare earth materials in doping silica to make fiber Lasers for industrial applications.
Chapter Three	Theoretical Framework: This chapter gave the underlying support structure or model for the study.
Chapter Four	Research Methodology: This chapter dealt with the methodology employed during model simulation and analysis.
Chapter Five	Data Presentation, Analysis and Discussion: This chapter dealt with the presentation of data, the analysis and the discussion of the findings.

Chapter Six	Conclusions and Recommendations: This chapter has presented conclusions and recommendations for the study.

1.10 Summary

Chapter one gave an overview of the study and its background. This chapter highlighted the fact that technology has taken center stage in easing Radar communication, Laser machining, Medical treatment of diseases, free space communication etc. This has been made possible due to the deployment of rare earth materials in the design of Lasers.

The next chapter, Chapter two, looks at how the rare earth materials, ytterbium in particular has been contextualized by looking at the earlier studies regarding the doping of silica with rare earth materials in designing Lasers for industrial application.

CHAPTER TWO

LITERATURE REVIEW

2.0 Introduction

This chapter reviews the theory and related works regarding design of ytterbium doped fiber lasers. The conceptualization of main concepts, related work studies, and rare earth element fiber doping laser experiences are presented in this Chapter in addition to a critique of the review followed by a summary of the entire chapter.

During the past sixty years, the progress of fiber lasers in terms of output powers and application has tremendously increased. Fiber lasers are known for their high average powers and beam qualities compared to other types of lasers. These features of doped fiber lasers are of importance to many industrial applications [30-31] which points to the reason of fiber lasers being one of the most important developments in laser technology [32]. This success can be attributed to the recognition of the use of fibers as both active media and waveguides in laser systems [7]. The flexibility of ytterbium ion in doped silica fibers is one of its strong points. Ytterbium ions exhibit strong scientific properties, particularly in its broad absorption band that ranges from slightly below 850 nm to more than 1070nm [33].

2.1 Main Concepts

Fiber lasers are adaptable to a lot of system configurations with different output features. A single mode fiber laser is capable of delivering power with excellent beam quality. A multimode fiber laser is equally capable of delivering much higher power compared to single mode fiber laser.

The following are the main concepts associated with fiber laser design particularly in the deployment of rare earth materials as dopants in the silica glass:

2.1.1 Laser Principles

A laser is created when the electrons in atoms in special glasses, crystals, or gases absorb energy from an electrical current or another laser and become excited. The Lasing process is made possible by three main components: A gain medium which can support a population inversion, an external exciter to create the population inversion in the gain medium and an optical resonator or cavity to create a high radiation density.

The three critical processes that take place in an active medium due to interaction of light and atoms are (i) absorption (ii) spontaneous emission and (iii) stimulated emission [34].

This can be depicted in figures 2(a), (2b) and (2c) below where only two energy levels E_1 and E_2 are considered for easy analysis.

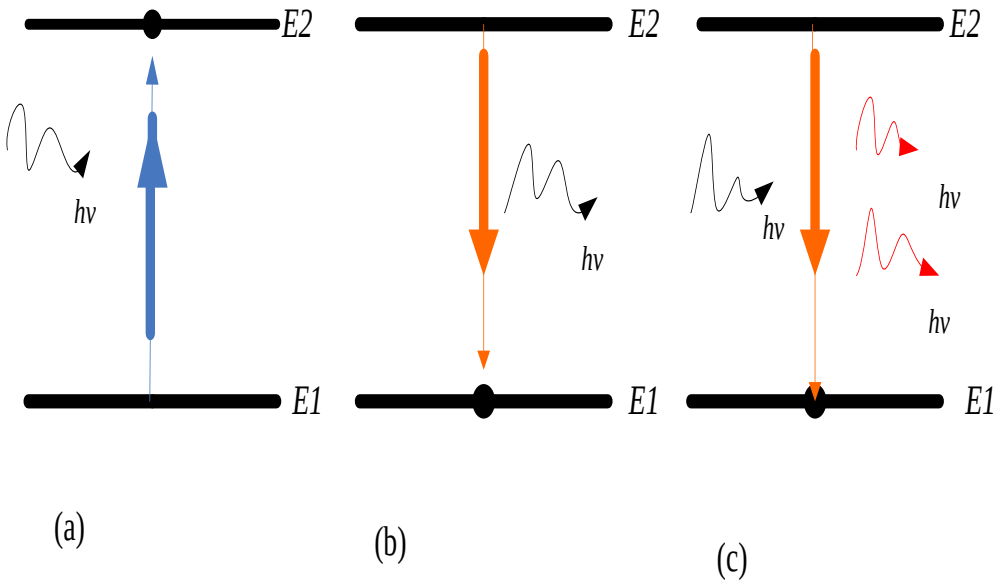

Figure 2: Depiction of lasing processes (a) absorption (b) spontaneous emission and (c) stimulated emission [34]

2.1.2 Absorption

Consider an atomic or molecular medium whose electrons are at ground state (E_1) as shown in figure 2(a). When a photon of frequency *v*, with energy *E* is incident on such a medium, the energy is transferred to the electrons which are then excited to a higher energy level, in this case, E_2

$$E = h\nu = E_2 - E_1 \quad (1)$$

Where: h=6.625 x 10-34j.s is the Planck's' constant

v is the frequency at which the electrons are excited to other energy levels.

This is the process of absorption and can result into population inversion. Population inversion is the state in which there are more electrons existing in the excited energy level compared to the ground state [34].

2.1.3 Spontaneous Emission

The excited electrons in figure 2(b) can return to the ground state without the influence of an external electromagnetic field, by emission of a photon. The atom will tend to decay to ground state as $E_2 > E_1$. This process is referred to as spontaneous emission. It occurs in all directions and results in spatially incoherent radiation in the medium.

2.1.4 Stimulated Emission

In contrast to the spontaneous emission, consider figure 2(c), when a photon of energy E interacts with the excited electron, a process similar but opposite to absorption occurs. During the interaction, an emission of additional photon with similar frequency, phase, polarization and direction as the incident photon occurs. At this point the incident wave is amplified [35]. This process is referred to as stimulated emission and was first described in [36]. Stimulated emission can only occur for incoming electromagnetic waves that have photon energy similar to the energy required for laser transition [35]. Normally, when a medium is fully engaged in a state of population inversion by pumping and an optical feedback is then provided by a resonator cavity, the stimulated emission can be amplified to produce a highly coherent beam of light.

2.1.5 The Laser Phenomenon

Considering the two energy levels of an assumed material shown in figure 2 and let N1 and N2 be the respective population levels of E1 and E2, the magnitude of the flux can be determined. The behavior of the material under normal and excited conditions is determined as:

When N2<N1, the material behaves like an absorber (normal condition)

When N2>N1, the material behaves like an amplifier (excited condition)

When N2=N1, the material is neither absorber nor amplifier (transparent condition)

2.1.6 Population Inversion

Under thermal equilibrium it is observed that N2<N1, which implies that the material behaves like an absorber. However, in a situation where N2>N1, the material acts like an amplifier and it is at this stage of behavior that population inversion is achieved in the cavity. Experimentally, the first concept of population inversion was done in 1954 [37]. In this experiment ammonia molecules produced emissions in the microwave region. In [38] a system was proposed for stimulation emission at infrared and optical wavelengths. In 1960, the first ever solid state laser in the optical range wavelength was demonstrated using a ruby crystal [39].

2.1.7 Laser cavity design

The fiber laser cavity has an active medium whose core has been doped with active ions such as erbium, neodymium, ytterbium etc. The cavity is formed by either use of bulk mirrors on either side of the fiber facets, or Fiber Bragg Gratings (FBG) written directly inside the fiber core. To achieve oscillation from an amplifier, a suitable positive feedback is critical. This is realized by situating the gain medium (active fiber cable) between highly reflecting mirrors. In this configuration as shown in figure 2.1 below, an electromagnetic wave travels in a direction orthogonal to the mirrors and bounces back and forth between the two mirrors [35].

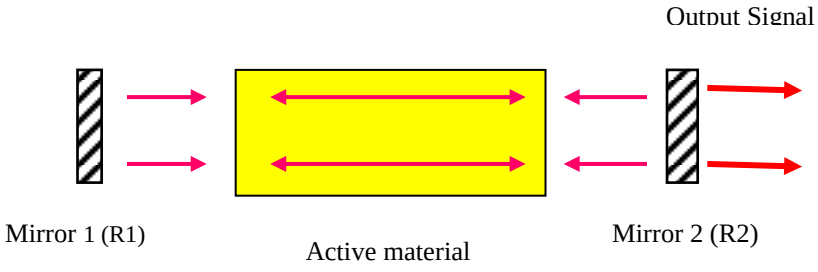

(a)

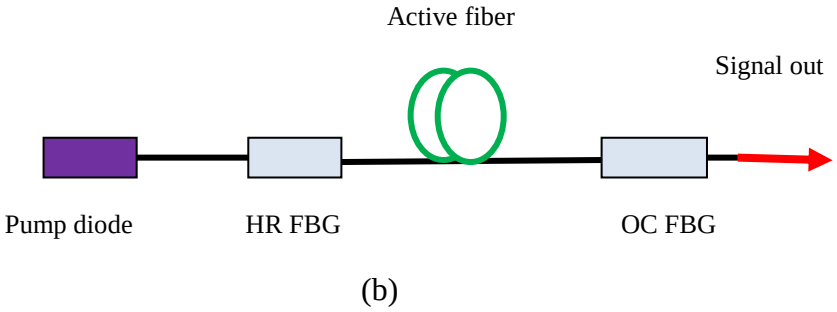

(b)

Figure 2.1: (a) Generic scheme of a Laser, (b) scheme of a fiber laser with FBGs as mirrors [35]

The signal is amplified on each pass through the gain medium. To extract useful laser beam from the cavity, one of the two high reflecting mirrors is made partially transparent. The two mirrors are referred to as HR usually with R >99% reflectivity, and OC usually with reflectivity (R) ranging from 5% to 80%. This helps to determine the output mode, either forward or backward mode power output. In lasers, oscillation starts when the gain of the active fiber material compensates the losses in the laser [34]. In Figure 2.1(a) setup, the pump is launched into both fiber ends through appropriately placed Dichroic mirrors (DM) that passes the signal and reflects the pump wavelengths. This configuration requires careful mirror alignment to avoid unwanted back reflections [40-41]. Such configurations are suitable for both high power lab demonstration [42-44] and low average power laser systems. Figure 2.1 (b) shows an all fiber pumped configurations where the bulk optic mirrors are placed by intra-core FBGs and the combined pumps are launched through the FBGs. This configuration adds extra stress on the FBGs as they are subjected to strong pump signal.

2.1.8 Pumping scheme

The term pumping is defined as the process of raising atoms from ground level to a higher level with the aim of achieving population inversion. Usually the pump sources are electromagnetic waves supplied to interact with the active material in the cavity. Pumping, for low power (milli-watt) fiber lasers, is done directly to the core of the laser.

For high power (watt to kilo-watt) fiber lasers, a double clad active fiber is used where pumping is launched in the inner cladding. The inner clad guides the pump beam which during the propagation crosses the active core and interacts with the doping material. Common pump schemes are side-pumping, end pumping and V-groove side pumping. The pump schemes can also be determined depending on the direction of pump propagation with regards to seed/laser propagation. In which case the pump schemes are classified as co-pumping, counter –pumping and bidirectional pumping.
These schematics are shown in figure 2.2 below.

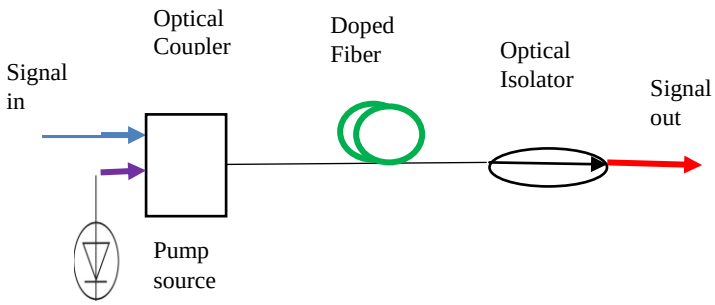

(a) Co-pumping

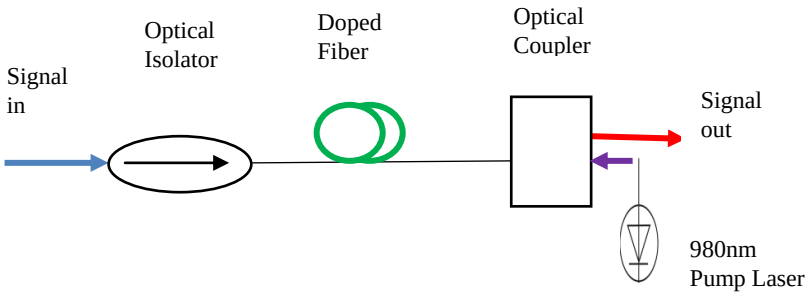

(b) Counter-pumping

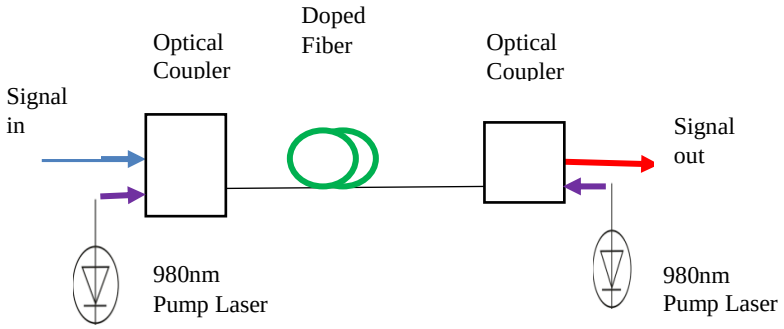

(c) Bidirectional-pumping

Figure 2.2: Three common pump schemes (a) co-pumping (b) counter-pumping and (c) bidirectional pumping

Co-pumping gives better noise performance and counter pumping allows higher gains. Bidirectional pumping takes the characteristics of the two pump schemes.

The optical coupler handles the combination of the pump and signal optical power for efficient input in the laser cavity or amplifier. The optical isolators prevent the amplified signal from reflecting back in the laser device to avoid an increase in the amplifier noise leading to decrease in the amplifier/laser efficiency.

2.1.9 Propagation modes

The two propagation modes in the optical fibers are single mode and multimode. Like any other transmission media, the performance and effectiveness of these modes of propagation are affected by attenuation and dispersion along the fiber cable [45]. The common attenuation mechanisms are absorptions, scattering, and radiative losses of the optical energy [46]. Dispersion is a consequence of factors such as intermodal delay, intra-modal dispersion, polarization mode dispersion and higher order dispersion effects. Operating modes of lasers are composed of longitudinal and transverse modes. The transverse modes are of critical use because it portrays the distribution of light intensity on the cross sections of the output laser beam. The preference on mode use in fiber lasers is single mode due its ability to handle high power levels.

2.2 Ytterbium Doped Fibers

2.2.1 Spectroscopic data for Yb^{3+} doped fibers

The flexibility of ytterbium ion in doped silica fibers is one of its strong points. Ytterbium offers a broad absorption band that ranges from slightly below 850nm to more than 1070nm because of the $^2F_{7/2}$ to $^2F_{5/2}$ transition as shown in its absorption spectrum in figure 2.4 [21]. Unlike the conventional solid state lasers counterparts, fiber lasers depicts numerous benefits notably enhanced conversion efficiency, high beam quality, high output power, high stability with temperature, etc. These features attracts many applications which include but not limited to radar, laser machining, free space communication and medical laser treatment. The broad absorption band allows for a wide choice of pump sources from a broad pump band. The broad pump band makes the consideration of pump wavelengths, pumping temperature and stability. Ytterbium doped silica has an impressive emission band that ranges from around 970nm to 1200nm [47]. Ytterbium ion does not have higher energy levels which significantly minimizes the occurrence of multi-photon relaxation as well as ESA. Ytterbium ions also have emission as well as absorption cross sections that are usually many times greater compared to rare-earth ions in multi-component glasses.

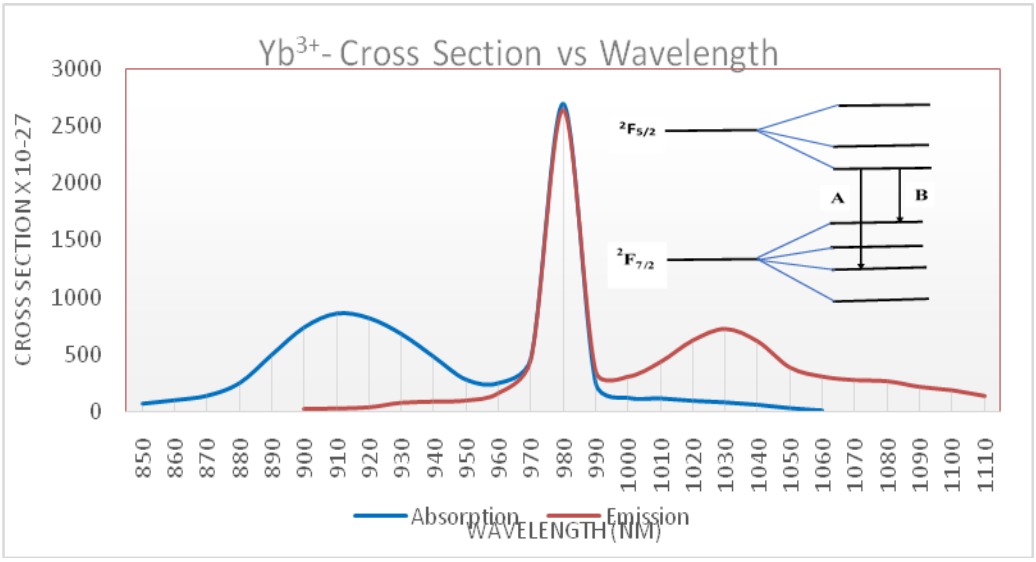

Fig 2.3: Ground-state absorption spectrum, emission spectrum, and energy diagram of Yb^{3+} in Silica [21].

2.2.2 **Energy level structure**

The Yb^{3+} ions electronic structure is shown in figure 2.4 below, with only the two main energy levels critical in the light amplification process, the lower manifold ($^2F_{7/2}$) and the upper manifold ($^2F_{5/2}$).

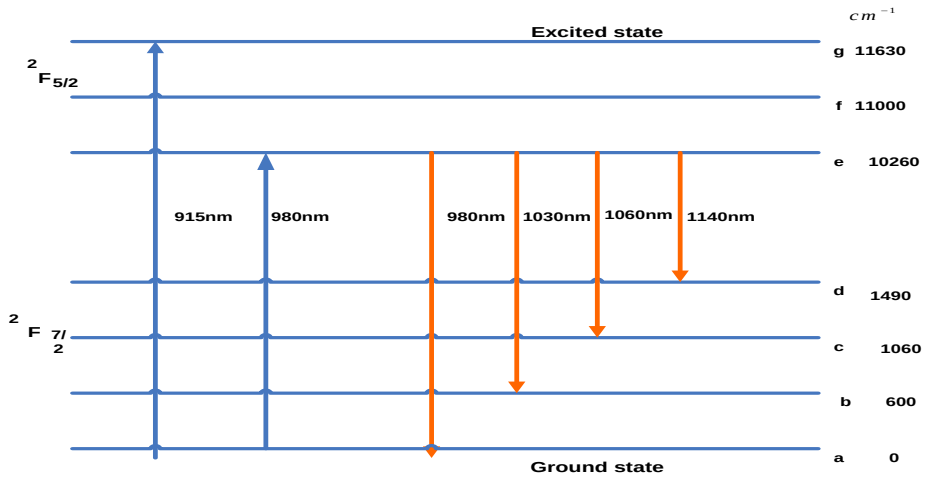

Figure 2.4: The Yb^{3+} energy level structure, consisting of lower manifold ($^2F_{7/2}$) and upper manifold ($^2F_{5/2}$) with their respective stark levels.

The consideration of rate equations is on the analysis based on the quasi-3 level which is exhibited by the Yb^{3+} ions as indicated in figure 2.4 above. The transition time between upper manifold and lower manifold for Yb^{3+} ions doped in silica host is approximately 880us. Ytterbium exhibits a quasi three level system at wavelengths pumping below 990nm and lasing wavelengths of around 1020nm to 1050nm [21]. In this study, pumping wavelength of 980nm, signal wavelength of 1018nm and pump power of 34watts in bidirectional pumping was considered. Figure 2.4 was analyzed to support the choice of the chosen wavelengths. With pump wavelength of 980nm, the transitions from upper manifold stark level e, the transitions can come to a or b of the lower manifold in the range of 980nm to 1030nm. Within this range of wavelength lasing, ytterbium exhibits quasi-three level system. The transitions can also be noticed from stark level e, to stark levels c or d of the lower manifold. These transitions in the lasing wavelength range of 1060nm to 1140nm exhibits quasi-four level system in the ytterbium ions. The transitions between the stark levels in each manifold are even shorter than the transitions between the upper and lower manifolds such that the Yb^{3+} ions in the fiber are effectively in either upper or lower manifold.

With this transition analysis, the gain medium may be modeled as a two level system as shown in figure 2.5(a) and figure 2.5 (b).

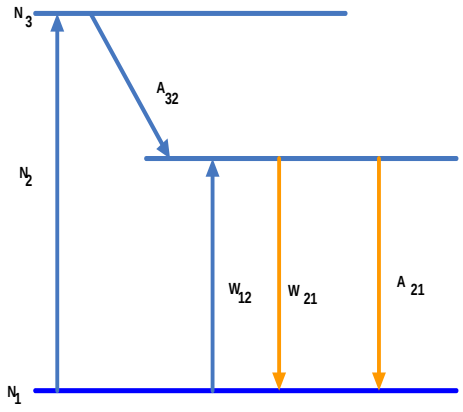

Figure 2.5 (a) Three level system

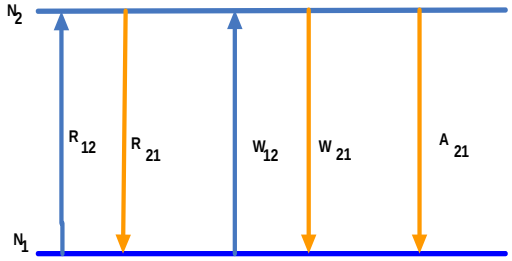

Figure 2.5 (b) Two level system

Formulation of Rate Equations for Yb^{3+} ions was done by considering the fact that only one excited state manifold is involved in the laser transition.

2.3 Laser Generation around 1018nm

Interest in development of YDFLs around 1018nm wavelength attracted wide research due to the performance of ytterbium ion in silica host [22]. Ytterbium doped glass exhibits unique and exciting features different from other rare earth materials. For instance, the simple energy level of ytterbium between the ground state and the meta-stable state reduces the ASE in the system. The atomic transitions between the sublevels in YDFLs, determines the pumping and laser amplification of YDFLs. Increasing the active fiber cable length of Yb^{3+} doped lasers affects the output of the laser negatively or positively. Apparently this is due to the three-level pattern of the energy level system [48]. Previous studies have shown that the wavelength can shift from 975nm in a 1m laser to slightly below 1100nm in a 100m laser [22]. Besides the basic characteristics of Yb^{3+}, the other factor contributing to the success of YDFLs is as a result of deploying double clad fiber technology in guiding the pump light in the active fiber [49-50]. The double clad pumping improves on the power scaling in doped lasers.

Power scaling is the process of power amplification due to varying of the pump power. Ytterbium-doped fiber lasers have a very exciting property of power scalability while maintaining excellent beam qualities. This is attributed to the

fact that Yb^{3+}doped fibers have a small quantum defect. The design of double clad fiber was first proposed in 1988 [49].

2.3.1 Double clad fibers (DCFs)

In cladding pumping, the pump power is coupled into the inner cladding of the active fiber [49] as shown in figure 2.6 below.

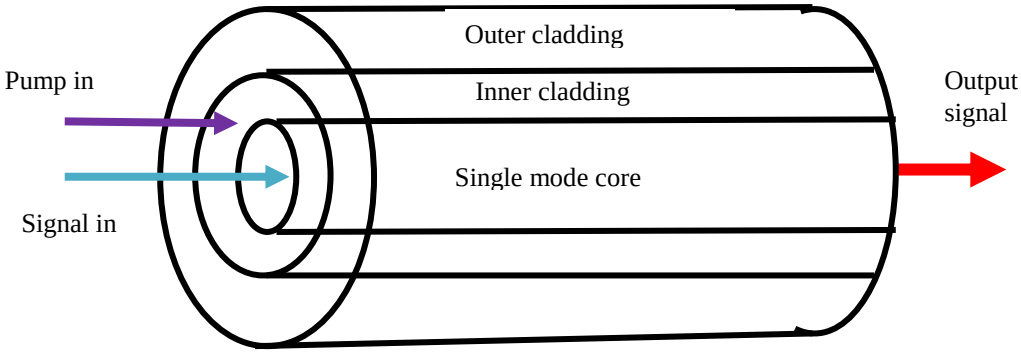

Figure 2.6: schematic of a double clad pumping scheme

The numerical aperture (NA) and diameter of the active core is smaller than the numerical aperture and diameter of the inner cladding. The light propagating in the inner cladding is refracted to the core and not vice-versa. It is guided into the inner cladding by total internal reflection. The pump light that interacts with the doped active core gets trapped in the core. Because of the smaller NA and diameter of the active core, the resulting output beam is much more bright and intense. Thus, clad pumping scheme is very powerful and efficient [51].

2.4 Development of 1018nm YDFLs

Development of YDFLs that operate around 1018 nm wavelength usually have a co-lasing around 1030nm. Therefore, the design has to take care of the ASE and ESA. The emission cross section around 1018nm is smaller in comparison to 1030nm. Therefore, the YDFLs operating below 1030nm face a challenge of gain competition between useful laser power and ASE [52]. To mitigate this challenge, the design has to ensure suppression on gain around 1030nm lasing. To achieve this, it is key to ensure that there is a high inner cladding to active core ratio relationship [52-53].

2.5 Related Works

Research studies aimed at establishing and designing of novel laser devices for industrial use has been the focus of research in the recent past. Light emitters (lasers) have been under investigation for a long time in improving the operations in domestic and industrial application. The laser design, using rare earth material, and application in industry has improved the services provided in terms of speed and quality. Investigated laser techniques include but not limited to doping with erbium (erb) [54], with Neodymium [55], using carbon dioxide [55], and using Helium neon gas [47]. These provide wide industrial usage such as bar code scanning, material cutting under garment fabrication, industrial steel cutting and welding and high speed communication. However, development of a novel laser device that meets the requirement of low dispersion, low noise figure, excellent energy confinement and effective beam to travel along distance is still lacking. For instance the use of erbium doped laser remarkably produced good power output but had a lot of noise in the system [54]. Too much pump power had to be pushed in the system to achieve a small reduction in the noise levels. In a related study, the use of Erbium doping on the Erbium doped fiber laser (EDFL) [56] provides excellent output power, achieves good noise suppression but it uses two laser sources which proves expensive to implement. A fiber laser is presented in [57], pumped at 970nm and lasing at 1018nm. With the pump power of 59.2W a lasing output power of 7.5W was achieved. The low power output was attributed to incomplete absorption of the pump power at 970nm pump wavelength. In [58], an Erbium co-doped with Ytterbium fiber laser device is presented. It produced an output power of 7.6watts against the pump power of 308watts at 1500nm wavelength. The difference between the pump power and the output power is huge an indication of poor efficiency. A fiber laser pumped at 976nm wavelength is presented in [59]. Pump power of 23W produced 13W in the seed laser. In the power scaling amplifier with pump power of 97W, the power output was 77W. The limitation observed was that there was too much unabsorbed pump power therefore recommended use of large full factor to improve the performance. In [60], a laser device pumped at 976nm and lasing at 1018nm is presented. With pump power of 435W a laser output of 309W was obtained representing slope efficiency of 71%. The performance was mainly controlled by effectively cooling the laser diodes in the pump circuit. The

recommendation was that cooling system should be improved in order to obtain best efficiency and also increase on the core/cladding ratio to suppress the unwanted ASE gain at 1030nm. A study in [61] presents a laser device pumped at 976nm with 140W pump power producing laser power of 105W at 1060nm wavelength. To improve the efficiency it was recommended that a highly Yb^{3+} doped active fiber laser with a large core/cladding ratio should be used. A fiber laser device in [62] is presented with pump power of 217W producing a laser output of 154W. This shows an efficiency of 71%. To achieve high efficiency, use of a shorter fiber cable is recommended. In a related study [63], a laser device is presented pumping at 976nm with pump power of 380W. A laser output power of 200W at 1018nm wavelength was obtained translating into 75% efficiency. The limitation observed in this study was insufficient pump power. A study in [64] presented a fiber laser device pump at 976nm with pump power of 168W. The laser produced laser output power of 126W at 1018nm wavelength representing 75% efficiency. The low efficiency is attributed to insufficient pump power. It is further recommended that a double pass pump configuration be used to attempt to realize good power scaling. In [65], a fiber laser is presented with pump power of 290W in a bidirectional pumping scheme. The device produced a laser output of 220W at lasing wavelength of 1018nm. The efficiency obtained of 75% could be improved by carefully optimizing the length of the doped fiber cable according to the observations on the limitations of the performance carried during the experiment. In another study [66], an ytterbium doped laser is implemented and produced 112 watts of laser output power against the pump power of 167 watts. This translates into 75% power efficiency. The device proved to be reliable. However, from the observations, it was recommended that the device needed more variations in the Yb^{3+} ion doping to improve the system further. In another study [67], an experiment is conducted with pump power of 320W producing a laser output power of 240W in forward pumping scheme. Core lasing was observed at 1025.3nm wavelength. The power efficiency obtained of 75% can be improved by deploying the FBG at the output coupler to significantly increase the round trip loss for the ASE. In [68], a high power 1018nm lasing wavelength ytterbium doped laser was deployed and produced 805watts of laser output power against pump power of 1200watts. The device deployed a co-pumping scheme.

The optical–to-optical efficiency of 64.9% was achieved by varying the length of the active fiber cable. This system can be improved by pumping more power as per

recommendation from the study conducted. Further, in the same study, the researcher attempted to design a fiber laser in bidirectional pumping scheme. A laser output power of 717W was obtained at pump power of 1114W. This translates into power efficiency of 64.4%. The challenges faced in the study were that the home made coupler had fabricating issues to do with reverse coupling and also fiber deformation. The researcher recommended refining of the technology of the coupler and also increasing the pump power in order to improve the device performance.

This study takes advantage of the limitations in the related works above and exceptional properties of Yb^{3+} to design a novel Yb^{3+} doped fiber laser for industrial application. A model has been designed to use Dichroic mirrors as opposed to using home-made couplers and FBG. Further, the model is pumped at 980nm wavelength as opposed to 976nm. The results of the new design were compared with the results in [68]. Additionally, based on the new model, a fiber laser device was designed with the following parameters: lasing wavelength of 1018nm, pump wavelength of 980nm, pump power of 68W in bidirectional pumping scheme, Dichroic coupler of HR=100% and OC=30%.

The related works attempted to analyze the parameters considered in the design of the fiber laser devices.

The following was a summary of the research findings in the related works:

Low pump power produces low laser output power and affects lasing, longer active fiber cables causes re-absorption in the laser device leading to low output power and Yb^{3+} ion concentration must be optimized for better laser output power.

2.6 Critique of the Literature

Design of fiber laser devices, just like most electronic devices, experiences complaints from the end users. The complaints suggest that the beam quality of the laser devices needs to be very good in order to help deliver good services in industrial applications. The literature reviewed suggests that a gap exist in any design and therefore there is room for onward improvement in the technology of fiber laser design. This study, however, was based on a theoretical modeling involving calculations using differential equations in an effort to obtain high power levels through optimizing the parameters such as pump power, active fiber cable length and ion concentration. The literature revealed that all the mentioned parameters are critical in the design of the fiber laser.

Further, the choice of the couplers for input and output parts is also critical in the design of the doped laser fiber. The greatest challenge, as reports indicated, is that it is not easy to get high power efficiency.

2.7 Summary

Progressive research has revealed that Yb^{3+}-doped laser materials operating at wavelengths around 1μm have been intensively investigated for a wide variety of applications not limited to, high-power and short-pulse lasers, material processing, and optical telecommunications [69-70]. Yb^{3+}ions are regarded as the main dopant for the applications because of their simple energy-level scheme that prevents excited state absorption [71].

This chapter reviewed the advancement in the design of Yb^{3+} laser device over the years. It showed the power scaling techniques used in different combinations of the parameters used in the designs.

The next chapter, Chapter Three, looks at the underlying support in terms of theoretical structure and conceptual framework for the study.

CHAPTER THREE

Yb^{3+} DOPED LASERS MODEL

3.0 Introduction

In this chapter, a theoretical model in CW, bi-directional pumping mode is designed.

3.1 Absorption and emission cross sections

All rare–earth–doped fiber amplifiers intensify the seed signal light through stimulated emission. The local rate equations describe the dynamics of the emission and absorption processes of doping ions within its host material by making use of its atomic energy structure as well as spectroscopic properties [72].

3.2 Rate Equations

With the introduction of the overlap factors and ignoring fiber losses, the simplified two level system rate equations and propagation equations are modeled as follows:

Figure 2.5 (a) in chapter two shows the arrangement of a quasi-three level and figure 2.5 (b) shows the arrangement for the Yb^{3+} ion with a two level system, for easy analysis of absorption and emission processes in the ytterbium doped laser. Three-level systems can be described using a reduced two-level model [73], when the non-radiative relaxations to the meta-stable state are extremely fast. At 980 nm pumping, the Ytterbium-doped gain medium can be modeled using a simple two level laser scheme shown in Figure 2.5 (b) in chapter two.

Formulation of Rate Equations for Yb^{3+} ions is done by considering the fact that only one excited state manifold is involved in the laser transition.

From figure 2.5 (b), the general absorption and emission expression is:

$$-R_{12}N_1 + R_{21}N_2 + W_{21}N_2 - W_{12}N_1 + A_{21}N_2$$

Grouping like terms

$$-(R_{12} + W_{12})N_1 + (R_{21} + W_{21} + A_{21})N_2$$

The relative population of Yb^{3+} ions in lower and upper energy levels is managed by the local rate equations and propagation equations given as follows [20].

$$\frac{dN_1}{dt} = -(R_{12} + W_{12})N_1 + (R_{21} + W_{21} + A_{21})N_2 \quad (2)$$

$$\frac{dN_2}{dt} = (R_{12} + W_{12})N_1 - (R_{21} + W_{21} + A_{21})N_2 \quad (3)$$

Where:

N_1 and N_2 are the normalized populations in the lower and upper energy levels

R_{12} and R_{21} are the pump excitations and de-excitation rates respectively

W_{12} and W_{21} are the signal absorption and emission respectively

A_{21} denotes the spontaneous emission rate

Considering the lower and upper energy levels and applying the law of energy conservation, equation in (4) is obtained. This equation is referred to as ion density equation that is given by [20].

$$N_1 + N_2 = N_t \tag{4}$$

Under steady state conditions:

$$\frac{dN_1}{dt} = 0 \quad , \quad \frac{dN_2}{dt} = 0 \tag{5}$$

Under steady state condition, equating (1) to 0, we have

$$0 = -(R_{12} + W_{12})N_1 + (R_{21} + W_{21} + A_{21})N_2$$

$$0 = (R_{12} + W_{12})N_1 - (R_{21} + W_{21} + A_{21})N_2$$

$$N_1 = \frac{(R_{21} + W_{21} + A_{21})N_2}{R_{12} + W_{12}}$$

$$N_1 = \frac{R_{21} + W_{21} + A_{21}}{R_{12} + W_{12} + R_{21} + W_{21} + A_{21}} \tag{6}$$

And,

$$N_2 = \frac{(R_{12} + W_{12})N_1}{R_{21} + W_{21} + A_{21}}$$

$$N_2 = \frac{R_{12} + W_{12}}{R_{12} + W_{12} + R_{21} + W_{21} + A_{21}} \tag{7}$$

The pump and signal transition rates in a fiber waveguide are determined from the absorption emission cross section of the ions in the host medium. These are written as:

$$R_{12} = \frac{\sigma_{R12} I_p}{h\nu_p} \tag{8}$$

$$R_{21} = \frac{\sigma_{R21} I_p}{h\nu_p} \tag{9}$$

$$W_{12} = \frac{\sigma_{W12} I_s}{h\nu_s} \tag{10}$$

$$W_{21} = \frac{\sigma_{W21} I_s}{h\nu_s} \tag{11}$$

Where:

I_p and I_s are the pump and signal power intensities respectively

ν_p and ν_s are the pump and signal transition frequencies respectively

h is the planks constant

σ_{R12} and σ_{R21} are pump absorption and emission cross sections respectively

σ_{W12} and σ_{W21} are signal absorption and emission cross sections respectively

And the spontaneous emission rate is given by:

$$A_{21} = \frac{1}{\tau} \tag{12}$$

Where: τ is the life time of Yb^{3+} ions in the excited state

3.3 Pump power and Signal power equations

This study considered Pump wavelength of 980nm and pump power of 34W

3.3.1 Pump power variations along the fiber is given by the propagation equation:

$$\frac{dP_{(980)}(z)}{dz} = \{(-\sigma_{R12}N_1 + \sigma_{R21}N_2)N_t\Gamma_{p(\lambda=980)} - \alpha_{p(\upsilon 980)}\}P_{(980)}(z) \tag{13}$$

Assuming no pump scattering losses ($\alpha_{p(\upsilon 980)}$), equation (13) becomes as:

$$\frac{dP_{(980)}(z)}{dz} = \{(-\sigma_{R12}N_1 + \sigma_{R21}N_2)N_t\Gamma_{p(\lambda=980)}\}P_{(980)}(z) \tag{14}$$

3.3.2 Considering Signal wavelength of 1018nm, Signal power variation along the fiber is given by the propagation equation:

$$\frac{dP_{(1018)}(z)}{dz} = \{(-\sigma_{W12}N_1 + \sigma_{W21}N_2)N_t\Gamma_{s(\lambda=1018)} - \alpha_{s(\upsilon 1018)}\}P_{(1018)})z) \tag{15}$$

Assuming no signal scattering losses ($\alpha_{s(\upsilon 1018)}$), equation (15) becomes as:

$$\frac{dP_{(1018)}(z)}{dz} = \{(-\sigma_{W12}N_1 + \sigma_{W21}N_2)N_t\Gamma_{s(\lambda=1018)}\}P_{(1018)}(z) \tag{16}$$

From the pump and signal propagation equations:

z denotes the active fiber length

N_1 and N_2 are the normalized population in the lower and upper energy levels

$\alpha_{p(\upsilon 980)}$ and $\alpha_{s(\upsilon 1018)}\}$ is the pump and signal scattering losses respectively

$\Gamma_{p(\lambda=980)}$ is the pump overlap factor defined as a ratio of pump core area over doped area

$\Gamma_{s(\lambda=1018)}$ is the signal overlap factor defined as the overlap of mode field area with doped area and N_t is the Rare Earth ion concentration.

From (16), the signal propagation equation, we get the small signal gain coefficient g(z) written as:

$$g(z) = (-\sigma_{W12} N_1 + \sigma_{W21} N_2) N_t \Gamma_{s(\lambda=1018)} \tag{17}$$

Where:

$\Gamma_{s(\lambda=1018)}$ is the signal overlap factor defined as the overlap of mode field area with doped area.

3.4 Theory of Fiber Laser

In designing of a linear cavity of a Yb^{3+} doped fiber laser, considering a two-level system and rate equations, two critical points have to be considered. Applying the boundary conditions of the cavity and setting the net round trip gain to unity. Figure 3 below shows the schematic of a Bi-directional-pumped linear cavity fiber laser.

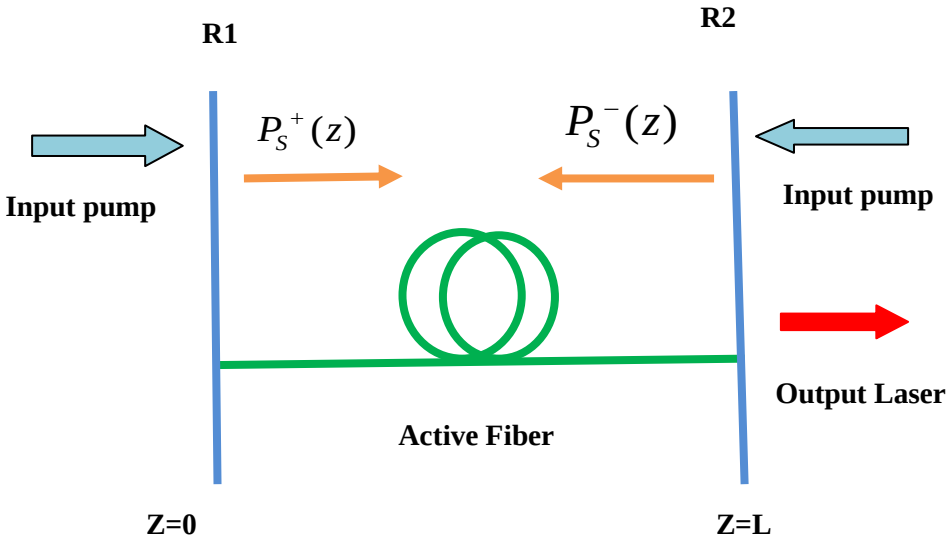

Figure 3: Schematic of Bidirectional pumped linear cavity fiber laser.

For Bidirectional propagating scheme, the gain, G, is obtained by integrating the gain coefficient in (17), over the length of the active fiber as:

$$G = \int_0^L g(z) dz$$

$$G = N_t \Gamma_s \int_0^L (-\sigma_{W12} N_1 + \sigma_{W21} N_2) dz \tag{18}$$

Considering the schematic drawing in figure 3.1 above, the boundary conditions for forward (P_S^+) and backward (P_S^-) propagating laser, respectively are given by [64]:

$$P_S^+(0) = R_1 P_S^-(0) \tag{19}$$

$$P_s^{-}(L) = R_2 P_S^{+}(L) \tag{20}$$

*R1*and *R2* are the power reflectiveness of the mirrors in the resonator cavity positioned at a distance of L apart. And then:

$$P_s^{-}(z) P_S^{+}(z) = \text{constant} \tag{21}$$

It is worth noting the stationary condition for a linear cavity fiber laser given as shown below;

$$R_1 R_2 \exp(2G) = 1 \tag{22}$$

For lasing to take place, the population in the N_2 must be more than the population in N_1 and this is achievable by ensuring enough gain and appropriate threshold power. Substituting equation (14) and equation (16) in equation (18) and applying the stationary condition given in (22), yields the gain and laser output power given as [74]:

$$G_p = \ln[P_p(L) / P_p(0)] \tag{23}$$

$$G_p = \frac{\Gamma_p \sigma_p}{2\Gamma_s \sigma_s} \ln(\frac{1}{R_1 R_2}) - \frac{\sigma_{w21}\sigma_{R12} - \sigma_{R21}\sigma_{W12}}{\sigma_S} \Gamma_p N_t L \tag{24}$$

And the absorbed pump power (Pa) is obtained as:

$$P_a = P_p(0) - P_p(L) \tag{25}$$

From (24), the laser output power is obtained as:

$$P_{out} = (1 - R_2) P_s^{+}(L)$$

$$P_{out} = \frac{\lambda_p}{\lambda_s} \frac{(1 - R_2) P_p{}^{sat}}{1 - R_1 - \sqrt{R_1 R_2} + \sqrt{R_1 / R}_2}$$

$$X[\frac{P_p{}^{+}(0) + P_p{}^{-}(L)}{P_p{}^{sat}} - (1 - \exp(G_P) - G_p - \Gamma_p N_t \sigma_{R12} L] \tag{26}$$

However, when power output is zero, $P_{out} = 0$, the laser threshold power is obtained as:

$$P_{th} = P_p{}^{sat} X \frac{G_p + \Gamma_p N_t \sigma_{R12} L}{1 + \exp(G_P)} \tag{27}$$

3.5 Theory of fiber Amplifier

Yb3+ doped fiber amplifiers operating at shorter wavelengths less than 1080nm are analyzed using two level model system [73], [75]. Effective use of reduced two model system is considered with certain assumptions such as:

Negligible power extracted by ASE. This is valid for fibers with input signal power significantly higher than the equivalent ASE noise in the gain medium. Secondly,

the dopant distribution and the field must not be non-homogeneous. This is valid for single mode doped fiber cores. And thirdly, Excited state absorption must not be present. This is true for Yb^{3+} doped fibers.

Considering the above assumptions, N_2 steady state population can be obtained from equation (7) - (11) as:

$$N_2 = \frac{\sigma_{R12}\sigma_s P_s{}^{sat} P_p + \sigma_{w12}\sigma_p P_p{}^{sat}(P_s)}{\sigma_p\sigma_s P_p P_s{}^{sat} + \sigma_p\sigma_s P_s{}^{sat}(P_s) + \sigma_p\sigma_s P_p{}^{sat} P_s{}^{sat}} \tag{28}$$

Where:

$P_p{}^{sat}$, is the pump saturation power (the power that reduces the absorption coefficient by a factor of 2 given as follows [74]:

$$P_p{}^{sat} = \frac{h\nu_p A}{\sigma_p \Gamma_p \tau} \tag{29}$$

$P_s{}^{sat}$, is the signal saturation power given by:

$$P_s{}^{sat} = \frac{h\nu_s A}{\sigma_s \Gamma_s \tau} \tag{30}$$

A, is the effective core area

$\sigma_p = \sigma_{R21} + \sigma_{R12}$, is pump attenuation coefficient

$\sigma_s = \sigma_{W21} + \sigma_{W12}$, is signal attenuation coefficient

Substituting equation (27) in the pump propagation equation (12) and signal propagation equation (13) and by integrating them over the length of the active fiber L, the coupled equation for the output pump and signal powers independent of propagation directions can be obtained as:

$$P_p{}^{out} = P_p{}^{in} \exp[-\sigma_p L + \frac{P_p{}^{in} - P_p{}^{out} + P_s{}^{in} - P_s{}^{out}}{P_p{}^{sat}}] \tag{31}$$

$$P_s{}^{out} = P_s{}^{in} \exp[-\sigma_s L + \frac{P_s{}^{in} - P_s{}^{out} + P_p{}^{in} - P_p{}^{out}}{P_s{}^{sat}}] \tag{32}$$

Roots to the Coupled equations can be found by using standard root finding techniques [76].

3.6 Reference model

In [28] a similar model, with output power of 717W at a launched pump power of 1114W, to this work was studied. Figure 3.1 below shows the reference model.

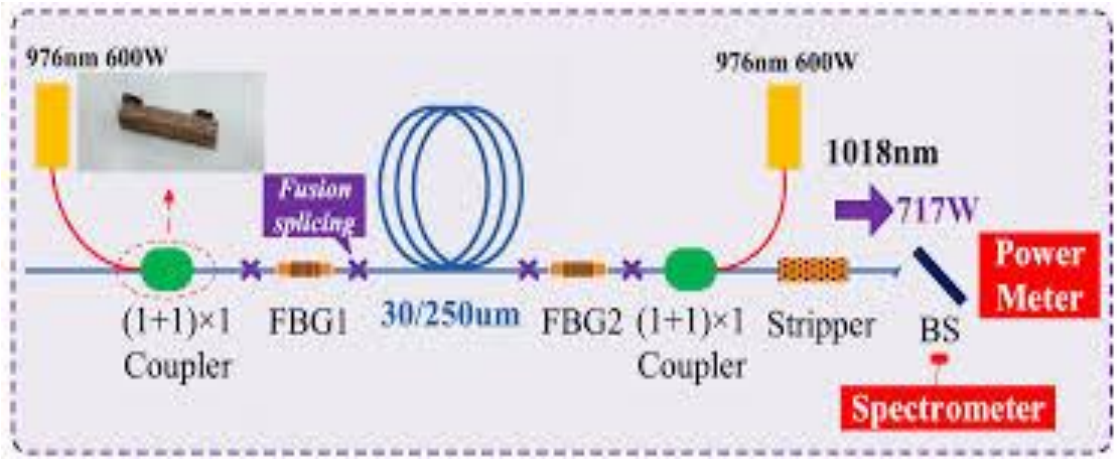

Figure 3.1: Experimental setup of the 1018nm YDFL pumped by 976nm LDs in Bi-directional pumping configuration [28]

The reference model above has the following limitations:

Challenges in fabricating homemade coupler in terms of tolerance of reverse coupling, challenges with fiber deformation, and challenges in high power handling especially at 30/250 micrometer

Arising from the challenges alluded to above, recommendations to improve output power were:

Refining the technology of the coupler and increasing the pump power.

This study took advantage of the gaps identified and used pump wavelength of 980nm as opposed to 976nm and also deployed Dichroic couplers as opposed to FBG.

Further, this work designed a completely new YDFL using pump wavelength of 980nm and pump power of 68W in bidirectional pumping scheme.

3.7 Summary

This chapter, chapter 3, revealed that Yb^{3+} doped lasers can be modeled from rate equations. Rate equations are powerful tools in that they aid in determining the propagations of the signal power as well as the pump power variations in the active fiber cable. Further, the rate equations help to determine the differential

equations to be calculated in order to achieve the best laser output power possible. The formulated gain equations and the output power equations shows how to optimize the device parameters such as the pump power, active fiber cable length and Yb^{3+} ion concentration levels in order to obtain good output power.

The next Chapter, Chapter four, looks at the methodology employed during the simulation of the model.

CHAPTER FOUR

RESEARCH METHODOLOGY

4.0 Introduction

This chapter outlines the method that was used in completing the study. It outlines the research design, and offers a description of how the simulation was conducted.

4.1 Research Design

In designing the Yb^{3+} doped Laser, a quantitative approach was used. Linear differential equations were solved in determining the variations in pump power, active fiber cable length and Yb^{3+} ion concentrations. The design was theoretical and implemented by use of computer software simulation. This was achieved through variations of the pump power to achieve an optimal level, variations of the active fiber length, and variation of the Yb^{3+} ions in the rare earth material in relation to the wavelength to achieve an optimal operation point. The three key parameter, pump power, active cable length and ytterbium ion concentration are critical in the design and must be optimized in order to achieve good slope efficiency. Pump power brings about photon absorption leading to spontaneous absorption and eventually stimulated emission. Varying the active cable length helps to determine how long the doped fiber cable shall be. A longer cable introduces re-absorption in the system and this lowers the system performance. The ytterbium ion concentration interacts with the light energy from the pump power and so if the concentration is poor, the photon released will not be fast enough to emit the energy required for stimulation in the cavity and this leads to poor performance in the system. Therefore, the three parameters play a very important role and must therefore be optimized if good laser designs have to be achieved. To effectively optimize the parameters, differential equations solved through Matlab brings out good results and hence the choice of using the adopted method.

4.2 Simulation Tools

In implementing our proposed model design of Yb^{3+} doped fiber laser, 7 enterprise, 64-bit operating systems, desktop computer with an Intel (R), core (TM) i5 CPU processor and 8GB Random Access Memory (RAM) will be used . The computer has been installed with MATLAB version 2018. This version of MATLAB has inbuilt laser MATLAB tools box functions to generate and propagate the test signal.

Further, MATLAB version 2018 was the only software package that could be afforded at the time of the research study period.

4.3 Simulation setup

The model described in chapter 3 was simulated with the help of a CODE in the Matlab. The CODE had a provision for input parameters such as the pump power, pump wavelength, signal or lasing wavelength, Yb ion concentration etc. The parameters are shown in table 4 below. Simulation was done in two parts. The first part involved comparison between a reference model done in [28] and a new (proposed) design. As seen from the table 4 below, the main difference was on the pump wavelength, 976nm and 980nm for the reference model and new model respectively. At 976nm pump wavelength, the waveband is too narrow and affects the stability of the signal. Unlike pumping at 976nm, pumping at 980nm wavelength has a wide waveband and has negligible fiber losses resulting into making the system to be stable. The other difference was on the cross section parameters in the pumping absorption and emission. Further, the Dichroic coupler was implemented as regards to FBG because the former is ideal for combining of two signals and the latter for combining of more than two signals. The comparison was done in order to determine the effectiveness of the code in comparing the results for the reference model to the new model.

The second simulation was done using the parameters shown in table 4.1. This was for a new model with pump power at 68W.

Table 4.0: Modeling Parameters for the reference model and a new model

		Reference model[28]	New model
Parameter	parameter symbol	value	value
Pump wavelength(nm)	λ_P	976	980
Signal Wavelength(nm)	λ_S	1018	1018
Core radius(μm)	Co_r	15	15
Clad radius (μm)	Cl_r	125	125
Numerical core aperture	NA core	0.08	0.08
Numerical clad aperture	NA clad	0.46	0.046
Yb3+ ion concentration (m^{-3})	Nt	1.00E+26	1.00E+26
pump overlap factor	Γ_P	0.0144	0.0144
signal overlap factor	Γ_S	1	1
signal absorption cross section-das	σ_{W12}	0.25e-26	0.25e-26
signal emission cross section-des	σ_{W21}	0.55e-24	0.55e-24
pump absorption cross section-dap	σ_{R12}	2.2e-24	2.1e-24
pump emission cross section-dep	σ_{R21}	2.1e-24	1.9e-24
active fiber cable length(m)	L	3	3
Pump power in(W)	Ppo	1114	1114
Highly reflective mirror	R1	0.995	0.995
output coupling mirror	R2	0.149	0.149
Excited state life time(ms)	A21	0.8	0.8

In order to achieve maximum laser output power from the model, parameters in tables 4.0 and 4.1 were used. The choice of 980nm pump wavelength and laser wavelength of 1018nm gives out the stable and wide absorption and emission cross section values as per ytterbium element characteristics. The core radius of 15*u*m and clad radius of 125*u*m gives an ideal numerical aperture of 0.08 and 0.46 respectively

for efficient operation of the laser. The pump overlap factor is the ratio of the core radius to the clad radius raised to the power of 2. The signal overlap factor of 1 is used in ytterbium doped laser assuming that there is no ESA and ASE in the system. The mirror reflectiveness of 0.995% and 0.145% for HR and OC respectively were used in this model since it falls within the recommended values in the design of YDFLs.

Table 4.1: Modeling Parameters for a new model pumped at 68W

		New Model
Parameter	parameter symbol	
Pump wavelength(nm)	λ_P	980
Signal Wavelength(nm)	λ_S	1018
Core radius(μm)	Co_r	15
Clad radius (μm)	Cl_r	125
Numerical core aperture	NA core	0.08
Numerical clad aperture	NA clad	0.046
Yb3+ ion concentration (m^{-3})	Nt	1.00E+27
pump overlap factor	Γ_P	0.0144
signal overlap factor	Γ_S	1
signal absorption cross section-das	σ_{W12}	0.25e-26
signal emission cross section-des	σ_{W21}	0.55e-24
pump absorption cross section-dap	σ_{R12}	2.1e-24
pump emission cross section-dep	σ_{R21}	1.9e-24
active fiber cable length(m)	L	0.5
Pump power in(W)	Ppo	68
Highly reflective mirror	R1	100%
output coupling mirror	R2	30%
Excited state life time(ms)	A21	0.8

Apart from some parameters which are common tables 4.0 4.1, the mirror reflectiveness of 100% and 30% for HR and OC respectively, were used in this model for maximum optimization. The active fiber cable length of 0.5m was chosen to ensure cable length reduction as compared to 3m used in the reference model. Further, pump power of 68W is ideal in radar, laser machining, free space communication and medical treatment.

4.4 Assumptions and Constraints

In designing the YDFL the following assumptions were made:

Negligible power extracted by ASE. This is valid for fibers with input signal power significantly higher than the equivalent ASE noise in the gain medium. Secondly, the dopant distribution and the field must not be non-homogeneous. This is valid for single mode doped fiber cores and thirdly, ESA must not be present. This is true for Yb^{3+} doped fibers.

4.5 Summary

In this study three variables were considered and varied to optimize the Laser output power. These were pump power, active cable length and Yb^{3+} ion concentration. Two simulations were done. One compared the existing model with the new model with the main difference being the pump wavelength. In the second simulation a new model was simulated with the pump source of 980nm and pump power of 68W in bidirectional pumping scheme. The results and findings are recorded in the next chapter, chapter five.

The next chapter, Chapter Five, looks at the data simulation results, analysis and discussion

CHAPTER FIVE

RESULTS, ANALYSIS AND DISCUSSION

5.0 Introduction

This chapter presents the results, result analysis and discussion using appropriate methods as explained under research methodology. The results are presented as results for simulation 1 and results for simulation 2. Results -1, is for the comparison of two models, one pumped at 976nm and the other pumped at 980nm. The results- 2 show the results for the new model according to this study pumped at 980nm with pump power source of 68W in a bidirectional scheme. Numerical modeling is carried out by solving the rate equations to study the effects of pump power, fiber length and Yb^{3+} ion concentration levels in the doped fiber. The other parameter of great importance is the application of the Dichroic mirror as opposed to Fiber Bragg grating.

5.1 RESULTS 1-Model comparison

5.1.1 Output Power with respect to Input pump power

Figure 5 shows the laser output power with respect to the pump power of 1114W launched into the active fiber from both ends of the cable. In [28] a similar arrangement was conducted to determine the optimal active fiber cable length.

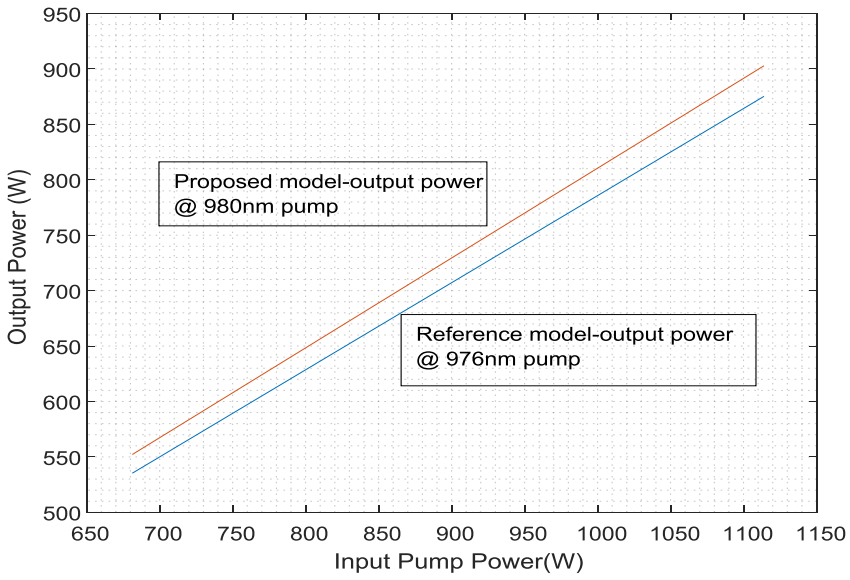

Figure 5: Modeling results of Laser output power vs. Input pump power

Laser output power of 902.86W at pumping power of 1114W was achieved through the simulation at the active cable length of 1.5m. The slope efficiency of output power to launched pump power was achieved at 81.05% as shown in figure 5. In a similar arrangement, pumping at 976nm, Laser output of 875.28W was obtained at 1.5m as shown in figure 5. The slope efficiency of 78.57% was achieved. The simulation at pump wavelength of 980nm shows better result than pumping at 976nm

5.1.2 Output power with respect to cable length

The active fiber cable was varied and the output power was obtained as shown in figure 5.1 below and further indicated in Table 5.

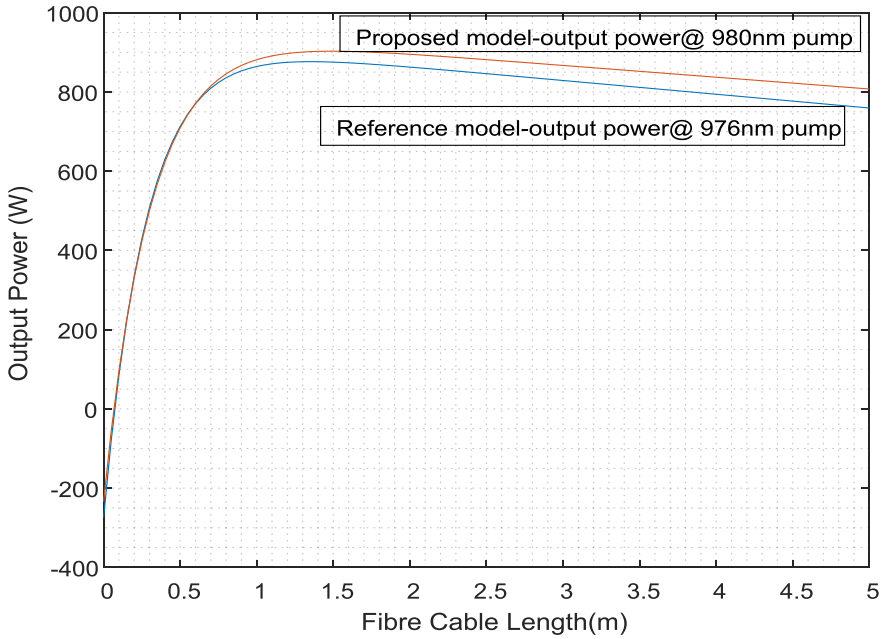

Figure 5.1: Modeling results of Laser output power vs. active fiber cable length

From figure 5.1, table 5 and figure 5.1.1 (a), at pump wavelength of 976nm, the laser output power at 1m active cable length was 864.3W. At 1.5m active cable length it increased to 875.28W and gradually started falling at 2m active cable length until it reached 759.5W at 5m active cable length. Clearly, the indication is that the optimum power was reached at 1.5m length with slope efficiency of 78.57%.

Table 5 shows the results in tabular form as extracted from figure 5.1 for easy checks at particular cable lengths. The results were obtained when OC was at 14.9% and the HR was at 99.5%. Another point to note is that the results obtained when the pump

wavelength was at 976nm are lower to the results obtained when the pump wavelength was set to 980nm.

Table 5: Output power with respect to active fiber cable length

Nt @1*e26 and OC reflectivity of 14.5%

Pump @976nm				
Fiber Cable length(meters)	Output power(W)	Pump power(W)	Efficiency (%)	comment
1	864.30	1114	77.59	
1.5	875.28	1114	78.57	
2	862.68	1114	77.44	Good output power
2.5	846.13	1114	75.95	
3	828.90	1114	74.41	In [28], output of 717 W@3m with efficiency @64.4% was achieved
3.5	811.57	1114	72.85	
4	794.21	1114	71.29	
4.5	776.85	1114	69.74	
5	759.50	1114	68.18	
Pump @980nm				
1	881.41	1114	79.12	
1.5	902.86	1114	81.05	Good output power at reduced cable length
2	895.05	1114	80.35	
2.5	881.54	1114	79.13	
3	866.92	1114	77.82	
3.5	852.08	1114	76.49	
4	837.21	1114	75.15	
4.5	822.32	1114	73.82	
5	807.43	1114	72.48	

The tabulated results in table 5 are further depicted in figures 5.1.1(a) and (b) to further demonstrate how different the results are between pumping at 976nm and 980nm in relation to the active fiber cable length.

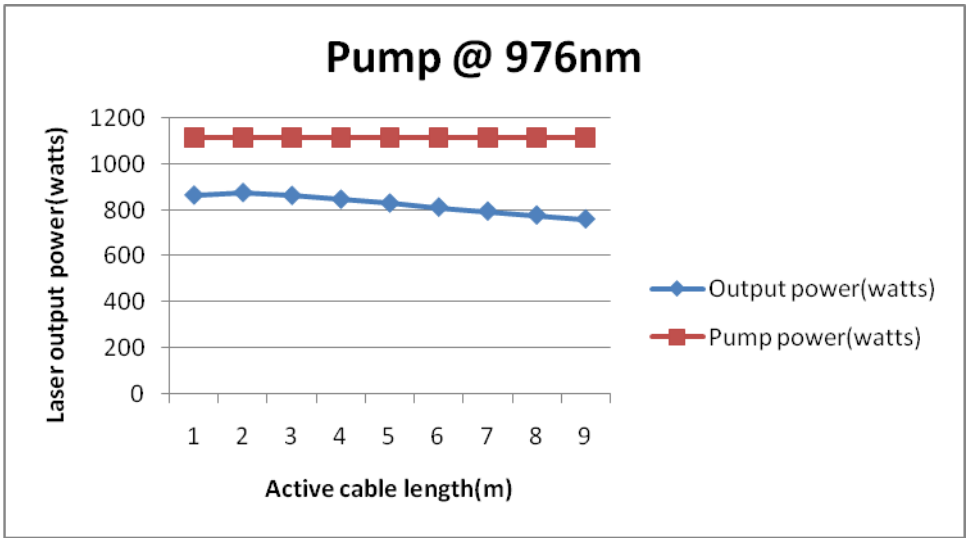

(a)

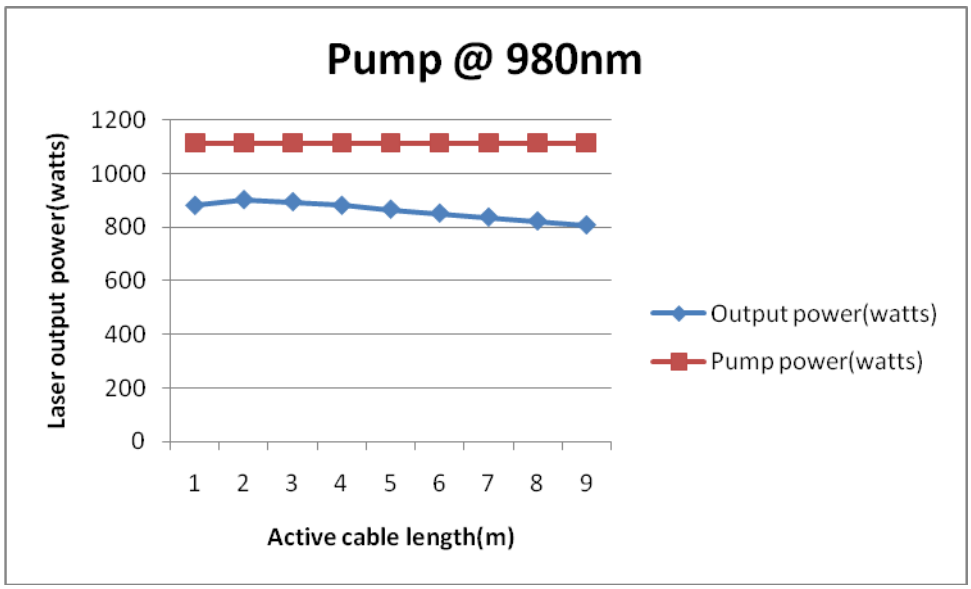

(b)

Figure 5.1.1: Modeling results (a) Laser output (W) at pump wavelength of 976nm, and (b) Laser output (W) at pump wavelength of 980nm

Similarly, from figure 5.1, table 5 and figure 5.1.1(b), at pump wavelength of 980nm, the laser output power at 1m active cable length was 881.41W. At 1.5m length it increased to 902.87W and gradually started falling at 2m active cable length until it reached 807.43W at 5m active cable length. Clearly, the indication is that the optimum power was reached at 1.5m length with slope efficiency of 81.05%. This means that using a longer active fiber cable is not profitable. In any case a shorter cable is ideal in that the cost is cheap and the device would be small in size.

As can be seen from table 5 and figure 5.1.1, active fiber length shorter than 1.5 m results in decreased laser output power. Longer fiber cable would excite re-absorption in the cable which may lead to parasitic lasing or photo darkening in the system. Therefore, in this simulation, the optimal fiber cable length is 1.5m. In the reference model [28], the best power output was 717W at a active cable length of 3m. However, in this study, at 3m the reference model has achieved 828.90W. This is possible looking at the assumptions made of no cable losses in the system. If the cables losses are factored in the output may be closer to 717W. This output indicates that the model in this study is really closer to what is obtaining in the modeling of the Yb^{3+} doped fiber lasers.

5.1.3 Output power with respect to wavelength

Figure 5.2 shows the relationship between the laser output power and the wavelength.

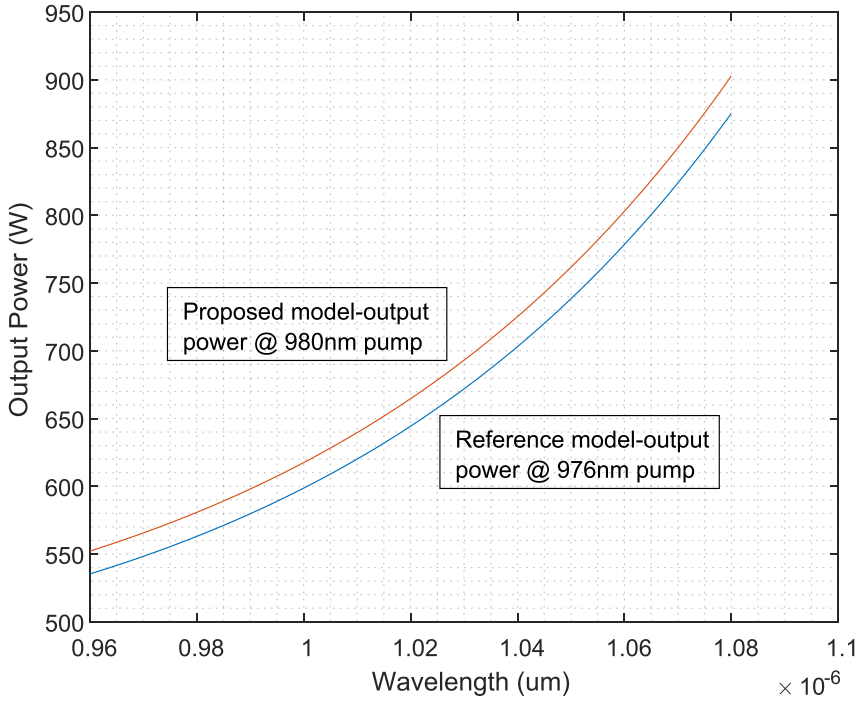

Figure 5.2: Modeling results of Laser output power vs. wavelength

As seen from figure 5.2 above, compared with YDFLs pumping at 976nm, pumping at 980nm showed high laser output power. Further, it can be seen that a shorter active fiber cable in relation to the pump wavelength is capable of producing a higher laser output power. This can be seen from table 5. To further optimize on the Laser output power, the parameters of the mirrors were adjusted. The OC mirror was set to 30%

and the HR mirror to 100%. A Dichroic coupler was deployed in this model. The simulation results are shown in table 5.1 below.

Table 5.1: Output power with respect to Active fiber cable length

Nt @1*e26 and OC reflectivity of 30%,HR of 100%

Fiber cable length(m)	Output power(W)	Pump power(W)	Efficiency (%)	comment
1	881.41	1114	79.12	
1.5	947.32	1114	85.04	Highest Laser power at reduced cable length
2	939.22	1114	84.31	

As seen from table 5.1 above, the result in this simulation with HR and OC mirror parameters of 100% and 30% respectively yields the highest laser output power. The active fiber cable length of 1.5m supports this good output.

5.1.4 Pump power with respect to active fiber cable length

The pump power along the fiber cable was completely absorbed at 1.5 m as shown in figure 5.3 below.

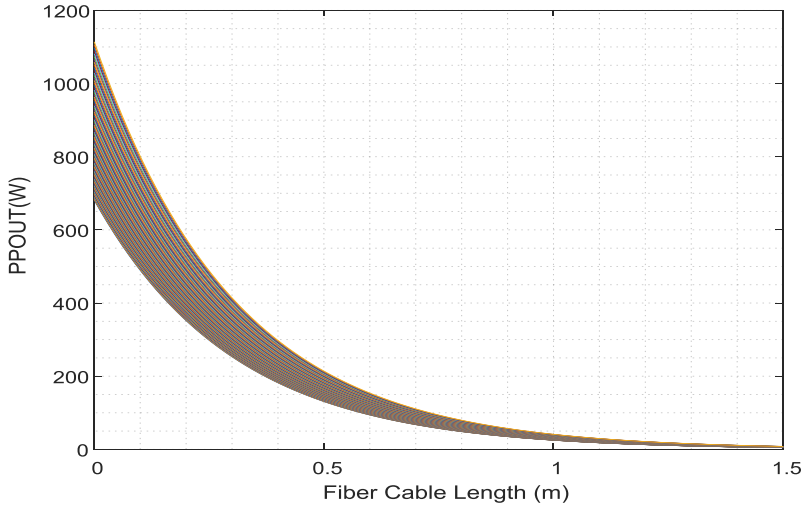

Figure 5.3: Pump power along the fiber cable

As seen from figure 5.3, pump power was completely absorbed in the active fiber cable at 1.5 m length. This shows that pumping at 980nm gives more Laser output power as compared to pumping at 976nm as shown in table 5.

5.1.5 Output power with respect to Yb^{3+} ion concentration

Figure 5.4 shows the relationship between the laser output power and the YB3+ ion concentration.

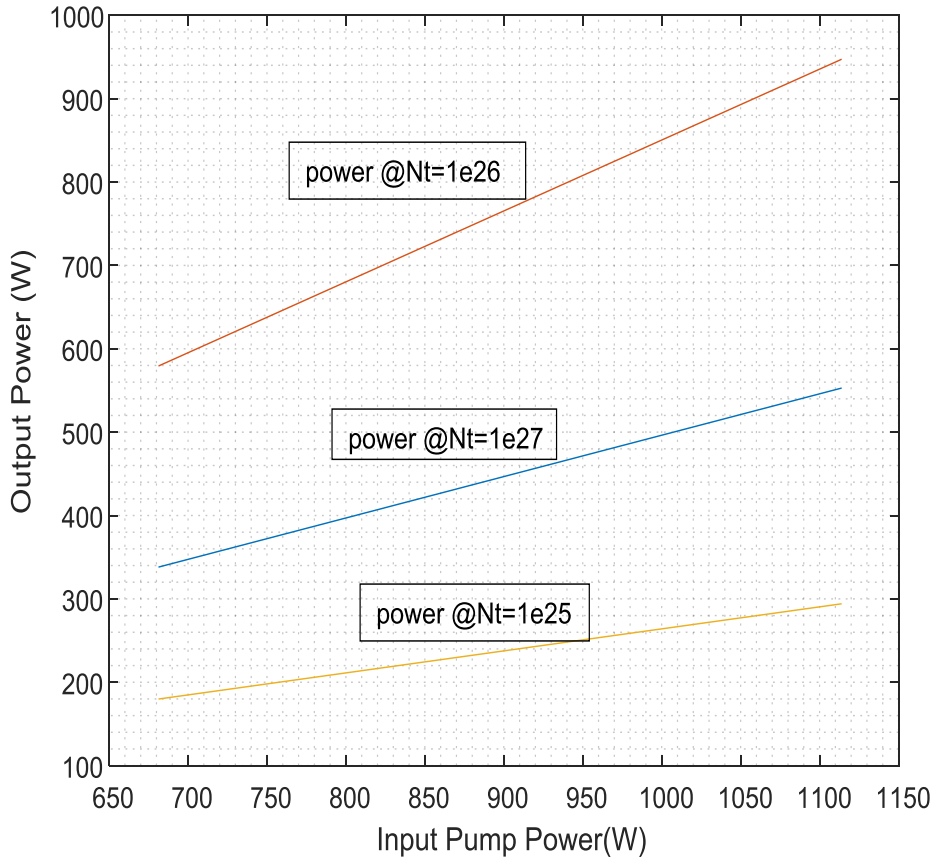

Figure 5.4: Modeling results of Laser output at Nt of 1e25, Nt of 1e26, Nt of 1e27 deploying HR of 99.5% and OC of 14.95%

Figure 5.4 above shows that variation in ion density concentration has an effect in the output power. From Figure 5.4 it can be seen that at Nt of 1e25, an output power of 223.47W is achieved. With the variation of ion density to Nt of 1e26, the power is 902.86W. At ion density of 1e27, the power output is 509.68W.

Comparing the three outputs at different ion densities, the output at 1e26 is optimized and gives the highest power. Clearly, it can be seen that the ion density

concentration is critical in fiber laser design. The modeling results are shown in table 5.2 below.

Table 5.2: Output power with respect to YB3+ Concentration@ HR=99.5% and OC=14.9%

Varying Nt, OC reflectivity of 14.9% ,HR of 99.5% and Cable length of 1.5m

YB3+ Concentration	Output power(W)	Pump power(W)	Efficiency (%)	comment
1e25	223.47	1114	20.06	
1e26	902.86	1114	81.05	Highest Laser power at reduced cable length
1e27	509.68	1114	45.75	

Compared with YDFLs set to HR and OC of 14.5% and 99.5% respectively, to further optimize on the Laser output power, the parameters of the mirrors were adjusted. The output coupling mirror was set to 30% and the highly reflective mirror to 100%. This is effective with deployment of Dichroic mirror. The simulation results are shown in figure 5.5 and in table 5.3 below.

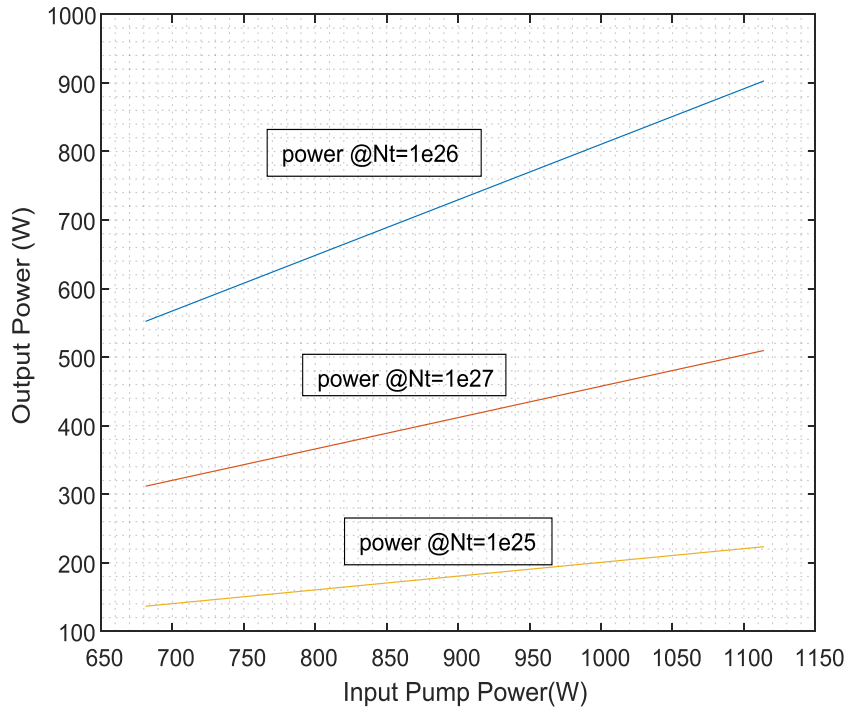

Figure 5.5: Modeling results (a) Laser output at Nt of 1e25, Nt of 1e26, Nt of 1e27 deploying HR of 100% and OC of 30%

Figure 5.5 above shows that variation in ion density concentration has an effect in the output power. From figure 5.5, at Nt of 1e25 an output power of 294.14W is achieved. With the variation of ion density to 1e26, the output power rises to 947.32W. At ion density of 1e27, the power output is 552.91W. Table 5.3 below shows the results from figure 5.5 in a table form for easy reference.

Table 5.3: Output power with respect to Yb^{3+} Concentration at HR=100% and OC=30%

Varying Nt, OC reflectivity of 30% ,HR of 100% and Cable length of 1.5m

YB3+ Concentration	Output power(W)	Pump power(W)	Efficiency (%)	comment
1e25	294.14	1114	26.40	
1e26	947.32	1114	85.04	Highest Laser power at reduced cable length
1e27	552.91	1114	49.63	

The results from the table above show that the Yb^{3+} concentration has a great effect on the laser output power.

5.1.6 Results- 1 summary

In this study the theoretical results were obtained based on the three variables. These were pump power, active fiber cable length and Yb^{3+} ion concentration. Maintaining the other parameters constant, the results revealed that pumping at 980nm yields higher power output compared to pumping at 976nm.

5.2 Results -2 results for a new model pumping at 980nm

The OC was set to 30% and the HR mirror to 100%. As opposed to deploying FBG, this model deployed Dichroic couplers. The simulation results are obtained per each parameter variation. The parameters varied are, pump power, active cable length and Yb^{3+} ion concentration levels in the active fiber cable.

5.2.1 Output Power with respect to Input pump power

Figure 5.6 shows the laser output power with respect to the pump power of 68wattts launched into the active fiber from both ends of the cable. Laser output power of 59.64W at pumping power of 68W was achieved through the simulation at the active cable length of 0.5m. The slope efficiency of output power to launched pump power was achieved at 87.71%.

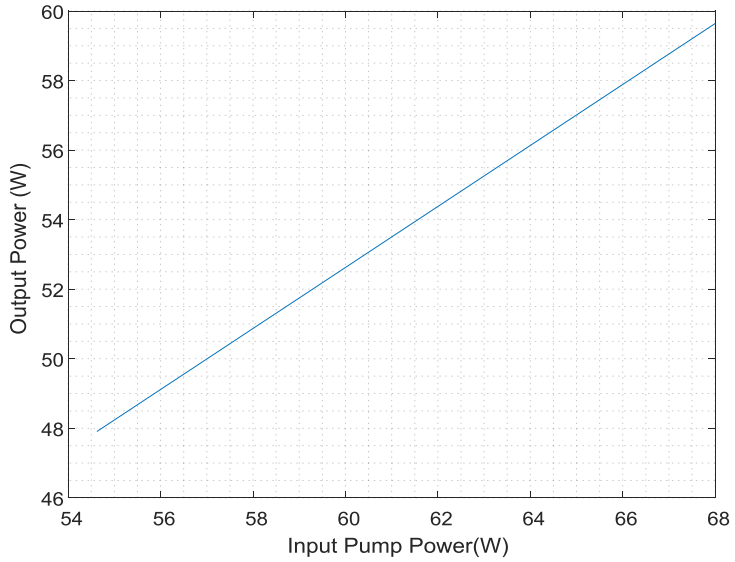

Figure 5.6: Pump power vs Input power

From figure 5.6 above , it can be seen that the maximum laser output power obtained showed good slope efficiency indication of low losses in the device. Further, figure 5.7 shows the graphs obtained in varying of pump power at three different levels.

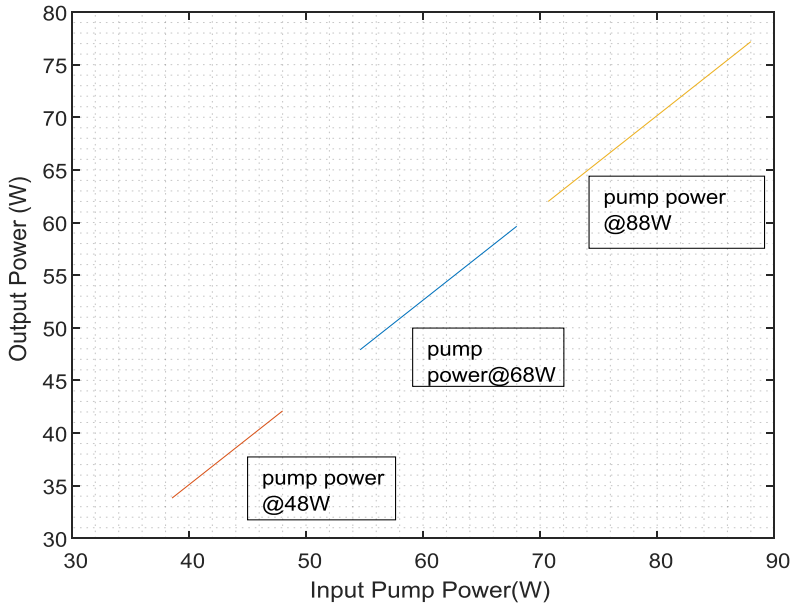

Figure 5.7: Modeling results (a) Laser output at pump power of 48W, 68W, and 88W

To further explain the graphs in figure 5.7 above, the results at three discrete pump power inputs thus 48W, 68W and 88W, have been well tabulated in table 5.4 below

for easy analysis. Keeping all other variables constant, varying the pump power gave the following laser output power:

Table 5.4: pump power vs. laser output power

pump power(W)	output power(W)	Efficiency (%)
48	42.10	87.71
68	59.64	87.71
88	77.18	87.71

From the table above it can be concluded that the variation on the pump power gave a good efficiency of 87.71%. This shows that the model is very efficient.

5.2.2 Output power with respect to cable length

The active fiber cable was varied and the output power was obtained as shown in figure 5.8 below and further indicated in Table 5.5.

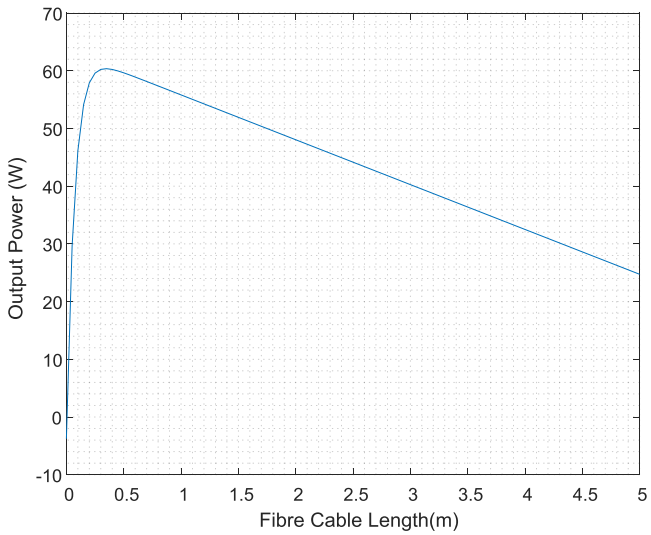

Figure 5.8: Active fiber Cable length vs. Laser output power

From figure 5.8, it can be seen that the highest output power was obtained at the cable length of 0.5m. Between 0 and 0.5m of the active fiber cable, the output will be low as the system requires to achieve a gain coefficient of zero at a particular point in the fiber. This means that a highest output power will only be achieved after the threshold value in which case the population inversion in lower state is less than the population inversion in the upper or excitation state. Figure 5.8 shows that the length of the active fiber cable should be optimized in order to get the best result in terms of

laser output power. The results in figure 5.8 can further be tabulated for easy analysis as shown in table 5.5 below.

Table 5.5: Output power with respect to active fiber cable length

Active fiber cable length(m)	Output power(W)	Pump power(W)	Efficiency (%)
0.5	59.64	68	87.71
1	55.82	68	82.08
1.5	51.93	68	76.37
2	48.05	68	70.65
2.5	44.16	68	64.94
3	40.27	68	59.23
3.5	36.39	68	53.51
4	32.50	68	47.79
4.5	28.61	68	42.08
5	24.73	68	36.36

From table 5.5 above, it can seen that the power output was highest, 59.64W, at 0.5m length representing slope efficiency of 87.71%, and started dropping gradually up to 24.73W at 5m active cable length with a representation of 36.36%. This means that the model has a good design of using a shorter cable length. This is very good in that it reduces the cost of the device. Further, this model will not encounter re-absorption in the laser device. It further means that the noise levels in the device will be negligible as per the assumption made of negligible ASE and ESA from the design perspective. The model shows that the device will work well up to 2.5m of active fiber cable. The tabulations of table 5.5 above can be seen in figure 5.9 below.

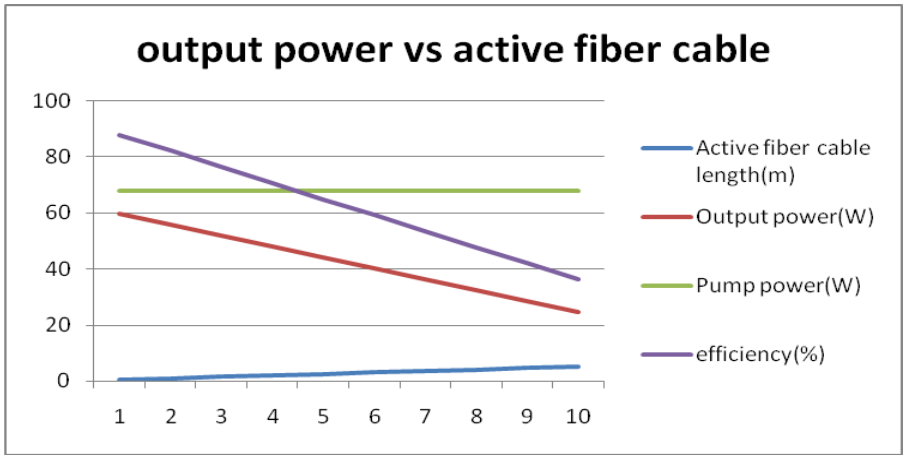

Figure 5.9: Output power efficiency of laser with varying active cable length

Figure 5.9 shows the output power of the laser which factors in other parameters such as efficiency in relation to other parameters.

It is evident from the results obtained with a shorter active fiber cable that longer active fiber cable would excite re-absorption in the cable which may lead to parasitic lasing or photo darkening in the system. Therefore, in this simulation the optimal fiber cable length is 0.5 m.

5.2.3 Output power with respect to wavelength

Figure 5.10 shows the relationship between the laser output power and the wavelength

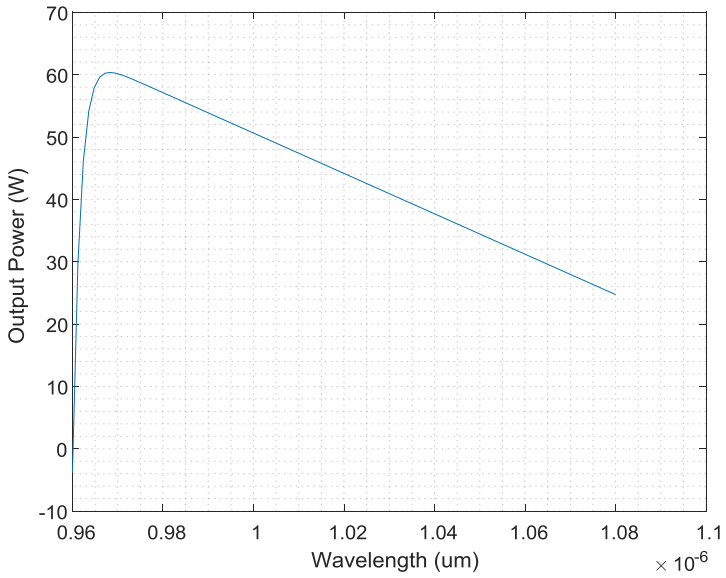

Figure 5.10: Wavelength vs. Output power @980nm pump wavelength

From figure 5.10 above, it can be seen that the output power reduces as the wavelength increases. This means that the longer wavelengths bring about re-absorption in the device and therefore, the wavelength must be chosen in such a way that it is not far from the pumping wavelength. The laser output will be achieved only if the population inversion in the excited state is higher than the ground state. This is also true in that the output power is only feasible if the laser wavelength is more than the pump wavelength. For wavelengths below 980nm in this modeling, there is no lasing because the pump wavelength is 980nm and therefore no laser output power is achieved.

5.2.4 Pump power with respect to active fiber cable length

The pump power along the fiber cable was completely absorbed at 0.5 m as shown in figure 5.11 below.

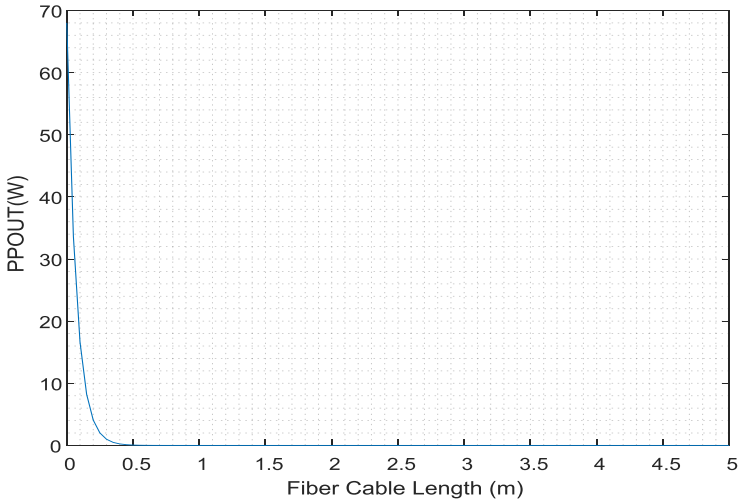

Figure 5.11: Pump power along the fiber cable

As seen from figure 5.11, pump power was completely absorbed in the active fiber cable at 0.5 m length. This means that the peak output laser power was achieved at active fiber cable length of 0.5m.

5.2.5 Output power with respect to Yb^{3+} ion concentration

Figure 5.12 shows the relationship between the laser output power and the Yb^{3+} ion concentration.

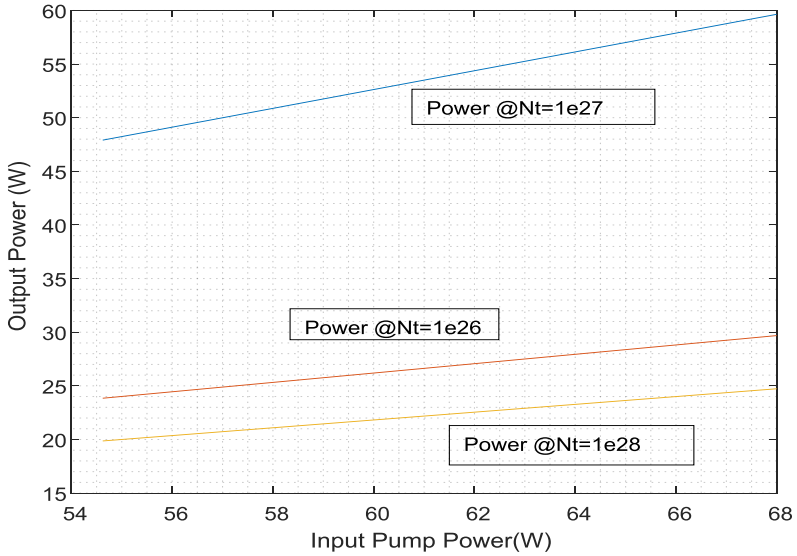

Figure 5.12: Modeling results Laser output at Nt of 1e26, Nt of 1e27, and Nt of 1e28 deploying HR of 100% and OC of 30%

Figure 5.12 above shows that variation in Yb^{3+} ion concentration has an effect on the output power. From figure 5.12, it can be seen that an output power of 29.69W was achieved at Nt of 1e26. With the variation of ion density to 1e27, the power was 59.64W. At Nt of 1e28, the power output reduced to 24.73W. This clearly shows that there is need to optimize the Yb^{3+} ion concentration in the design of the Yb^{3+} doped fiber lasers. Highly doped lasers perform well in shorter active cables. Bidirectional pumping scheme used in this model helps to ensure quick absorption takes place in the active laser fiber thereby reducing on the noise in the laser device. Table 5.6 below further shows the effect of the Yb^{3+} concentration in the doped laser fiber.

Table 5.6: Output power with respect to Yb^{3+} Concentration

Varying Nt ,OC reflectivity of 30%,HR of 100% and cable length of 0.5m

Yb^{3+} Concentration	Output power(W)	Pump power(W)	Efficiency (%)	comment
1e26	29.69	68	43.66	
1e27	59.64	68	87.71	Good output power
1e28	24.73	68	36.37	

From table 5.6 above, it can be seen that the best output power was at Yb^{3+} concentration of, Nt = 1e27. The results from the simulations indicate that the range of 1e26 to 1e28 will produce a peak output power at a discrete value of 1e27. The doping level of the ion concentration is done homogeneously along the fiber cable and this therefore means that at any particular point, simulation considers only one value of the doping in the propagation equation.

5.2.6 Results -2 summary

From the simulation results-2 of the new model, it can be seen that the design parameters plays a critical role in ensuring that the power output is achieved. Attention has to be put in optimizing the pump power, active cable length and Yb^{3+} concentration in order to have a good performing laser device.

5.3 Summary

In this study the theoretical results were obtained based on the three variables. These were pump power, active cable length and Yb^{3+} ion concentration. The results showed that the three variables were critical in determining the optimal output power of the fiber Laser. The results-1 on the comparative study showed that pumping at 980nm as opposed to 976nm gave good laser output power. Further, the results-2 on the new model gave very good efficiency of 87.71%.

The next chapter, chapter Six, looks at the conclusion and recommendations of the study.

CHAPTER SIX

CONCLUSIONS, RECOMMENDATIONS AND FUTURE WORKS

6.0 Introduction

In this chapter, the summary of, findings and conclusions from the entire study have been presented followed by recommendations arising from the study.

6.1 Conclusions

Fiber laser devices based on Yb^{3+} ions are of particular interest in industrial applications due to unique advantages possessed by ytterbium. The study modeled an YDFL pumping at 980nm in bidirectional mode. From the results obtained it is seen that:

i. The study achieved highest laser output power of 59.64W when 68W of pump power was launched into the cavity. This translates into 87.71% slope efficiency.
ii. The study achieved highest output power of 59.64W at an active fiber cable length of 0.5m.
iii. The study obtained highest output power of 59.64W at an Yb^{3+} ion concentration of 1e27.
iv. Further, the study revealed that, the Dichroic coupler of HR of 100% and OC of 30% obtained laser output power of 947.32W compared to the output power of 902.86W at HR and OC of 99.50% and 14.95% respectively.

Arising from the results obtained and considering the objectives guiding this research study, it can be concluded that:

i. Increase in the pump power increases the laser output power.

   As seen from the results obtained. When the pump power was varied from 0 to 68W, the laser output power increased and reached an optimal value of 59.64W in relation to peak value of pump power of 68W.
ii. Increase in the fiber cable length reduces the laser output power.

   From the results obtained when the active fiber cable was varied, highest laser output power of 59.64W was achieved at 0.5m of active fiber cable. As the active fiber cable was varied beyond 0.5m, the output power

started dropping gradually until it reached 24.73W at active fiber cable length of 5m.

iii. Lower ion concentration reduces the laser output power and consequently, higher ion concentration reduces the laser output power. From the results obtained, laser output power of 29.69W, 59.64W and 24.73W was achieved at Nt of 1e26, 1e27 and 1e28 respectively. This clearly shows that the ion concentration has an effect on the laser output power.

iv. Additionally, it can be concluded that the choice of the reflectivity is critical in the design as seen when HR of 100% and OC of 30% was used. This combination gave out the highest output power.

6.2 Recommendations

Arising from this study we propose the following recommendations:

Firstly, we note the good results achieved based on this theoretical model and therefore propose that the doped laser be actualized into a finished product and be implemented in industry.

Secondly, when designing doped laser devices, the critical parameters thus: pump power, active cable length and ion concentration should be varied until an optimal point is reached. The systematic variation of parameters helps the designers to come up with good products.

6.3 Future Works

Future works must consider further study of this proposed model by conducting experiments to see if the theoretical results will match with the experimental results.

Secondly, a study of the co-doped fiber deploying ytterbium and any other element from the rare earth elements such as Neodymium should be modeled to see if the results improve further in terms of fiber cable length.

6.4 Summary

This Chapter has given major conclusions, recommendations and suggested future work in the Laser industry.

REFERENCES

[1] Dowden, J. The Theory of Laser Materials Processing: Heat and Mass Transfer in Modern Technology. Berlin: Springer Science & Business Media (2009)

[2] C. Jauregui, J. Limpert, and A. Tünnermann, Nat. Photonics 7, 861 (2013).

[3] V. R. Supradeepa and J. W. Nicholson, Opt. Lett. 38, 2538 (2013).

[4] W. Shi, Q. Fang, X. Zhu, R. A. Norwood, and N. Peyghambarian, Appl. Opt. 53, 6554 (2014).

[5] E. Snitzer, "Proposed fiber cavities for optical masers," Journal of Applied Physics, vol. 32, no. 1, pp. 36–39, (1961).

[6] J. Cesar, L. Jens, and T. Andreas, "High-power _fiber lasers," Nature Photonics, vol. 7, (Nov 2003).

[7] E. Snitzer, "Neodymium glass laser," in Quantum Electronics, vol. 1, p. 999, (1964).

[8] R. J. Mears, L. Reekie, I. M. Jauncey, and D. N. Payne, "Low-noise Erbium doped fiber amplifier at 1.54 _m," Electronics Letters, vol. 23, no. 19, pp. 1026–1028, (1987).

[9] D. C. Hanna, R. M. Percival, I. R. Perry, R. G. Smart, P. J. Suni, J. E. Townsend, and A. C. Tropper, "Continuous-wave oscillation of a mono mode Ytterbium-doped fiber laser," Electronics Letters, vol. 24, no. 17, pp. 1111–1113, (1988).

[10] D. J. Richardson, J. Nilsson, and W. A. Clarkson, "High power fiber lasers: Current status and future perspectives [Invited]," *J. Opt. Soc. Amer. B,* vol. 27, no. 11, pp. B63–B92. (2010)

[11] Pask HM, Carman RJ, Hanna DC et' al."Ytterbium-doped silica fiber lasers: versatile sources for the 1–1.2 μm region," IEEE J. Sel. Top. Quantum. Electron. 1, 2-12, (1995)

[12] Paschotta R, J. Nilsson, A. C. Tropper, and D. C. Hanna, "Ytterbium-doped fiber amplifiers," IEEE J. Quantum. Electron. 33, 1049-1056, (1997)

[13] Nilsson J, Sahu J.K, Jeong Y, Clarkson A, et 'al,"High power fiber lasers," Proc. SPIE 4974, 50-59. (2003)

[14] H. Xiao, J. Leng, H. Zhang, L. Huang, J. Xu, and P. Zhou, "High-power 1018 nm ytterbium-doped fiber laser and its application in tandem pump," Appl. Opt. 54, 8166–8169, (2015).

[15] E. Stiles, “New developments in IPG fiber laser technology,” in 5th International Workshop on Fiber Lasers, (2009).

[16] X. Qi, S.-P. Chen, H.-Y. Sun, B.-K. Yang, and J. Hou, “1016nm all fiber Pico-second MOPA laser with 50W output,” Opt. Express 24, 16874–16883 (2016)

[17] X. Du, H. Zhang, H. Xiao, P. Zhou, and Z. Liu, “Temporally stable random fiber laser operates at 1070 nm,” IEEE Photon. J. 7, 1503107 (2015).

[18] C. Ottenhues, T. Theeg, K. Hausmann, M. Wysmolek, H. Sayinc, J. Neumann, and D. Kracht, “Single-mode monolithic fiber laser with 200 W output power at a wavelength of 1018 nm,” Opt. Lett. 40, 4851–4854, (2015).

[19] Y. Glick, Y. Sintov, R. Zuitlin, S. Pearl, Y. Shamir, R. Feldman, Z. Horvitz, and N. Shafir, “Single-mode 230 W output power 1018 nm fiber laser and ASE Competition suppression,” J. Opt. Soc. Am. V.33,no.7,pp. 1392–1398, (2016).

[20] Fady. I, et’al” Temperature Dependency of Ytterbium-Doped Fiber Laser (YDFL) Based on Fabry-Perot Design Operating at 915 nm and 970 nm High Power Pumping Configuration”JERT, volume.3, no.1, pp.1748, (2016)

[21] Pask HM, Carman RJ, Hanna DC et. al. “Ytterbium-doped silica fiber lasers”: Versatile sources for the 1–1.2 μm region, *IEEE J. Select. Top. Quant. Electron*, 1 (1): 2- 13, (1995)

[22] R. Paschotta, J. Nilsson, P. Barber, J. Caplen, A. Tropper, and D. Hanna, “Lifetime quenching in yb-doped fibres," Optics Communications, vol. 136, No. 5, pp. 375-378, (1997).

[23] R. Paschotta, Article on "quantum defect" in the encyclopedia of laser Physics and technology" ,(Oct 2008).

[24] Jeong, Y.-C., Boyland, A. J., Sahu, J. K., Chung, S.-H., Nilsson, J., & Payne, D. N., “Multi-kilowatt Single-mode Ytterbium-doped Large-core Fiber Laser”. Journal of the Optical Society of Korea, 13(4), 416–422, (2009)

[25] L. Huang, W. Wang, J. Leng, S. Guo, X. Xu, and X. Cheng, “Experimental investigation on evolution of the beam quality in a 2 kW high power fiber amplifier,” IEEE Photon. Technol. Lett.vol. 26, pp.33–36, (2014).

[26] T. Sakimura et al., “1.5-μm high-gain and high-power laser amplifier using a Er, Yb: glass planar waveguide for coherent Doppler lidar,” in Proc. CLEO, San Jose, p.114,(2012).

[27] T. Muangpool, S. Pullteap, "Reviews on laser cutting technology for industrial applications," Proc. SPIE 10714, Third International Conference on Photonics Solutions (ICPS2017), 107140Q, (5 March 2018).

[28] Yakup Midilli, O. Benjamin Efunbajo, Bartu şimşek, and Bülend Ortaç, "1018 nm Yb-doped high-power fiber laser pumped by broadband pump sources around 915 nm with output power above 100 W," Appl. Opt. 56, pp. 7225-7229, (2017).

[29] Ping Yan, Xuejiao Wang, Dan Li, Yusheng Huang, Junyi Sun, Qirong Xiao, and Mali Gong, "High-power 1018 nm ytterbium-doped fiber laser with output of 805 W," Opt. Lett. 42, pp.1193-1196, (2017).

[30] C. Labaune, D. Hulin, A. Galvanauskas, and G. A. Mourou. On the feasibility of a fiber-based inertial fusion laser driver. Optics Communications; 281(15–16): 4075–4080, (2008).

[31] G. Mourou, B. Brocklesby, T. Tajima, and J. Limpert," The future is fibre Accelerators". Nature Photonics; 7: pp.258–261, (2013)

[32] J. Cesar, L. Jens, and T. Andreas, "High-power fibre lasers," Nature Photonics, vol. 7, Nov (2003).

[33] H. Xiao, J. Leng, H. Zhang, L. Huang, J. Xu, and P. Zhou, "High-power 1018 nm ytterbium-doped fiber laser and its application in tandem pump," Appl. Opt., vol. 54, pp. 8166-8169, (Sep 2015).

[34] S. Orazio, "Principle of lasers," (1989).

[35] R. Paschotta, "Field guide to lasers," (2007).

[36] A. Einstein, "On the quantum theory of radiation," Physikalische Zeitschrift, vol. 18, pp. 121–128, (1917).

[37] J. P. Gordon, H. J. Zeiger, and C. H. Townes, "Molecular microwave oscillator and new hyperfine structure in the microwave spectrum of NH3," Physical Review, vol. 95, no. 1, pp. 282–284, (1954).

[38] A. L. Schawlow and C. H. Townes, "Infrared and optical masers," Physical Review, vol. 112, no. 6, p. 1940, (1958).

[39] T. H. Maiman, "Stimulated optical radiation in ruby," Nature, vol. 187, pp. 493–494, (1960).

[40] J. Limpert *et al.*, *Appl. Phys. B* 75, 477, (2002).

[41] S. Bohme *et al.*, *Proc. SPIE* 8244, 824406, (2012).

[42] Y. Jeong, J. K. Sahu, D. N. Payne and J. Nilsson, *Opt. Express* 12, 6088 ,(2004).

[43] C.-H. Liu *et al.*, *Electron. Lett.* 40, 1471, (2004).

[44] J. Nilsson *et al., Opt. Fiber Technol.* 10, 5, (2004).

[45] V. Alawin, "Optical network design and implementation", Mar 2004.

[46] K.Tsujikawa, K.Tajima, and J.Zhou,'intrinsic loss of optical fibers'Optical Tech., vol.11, no.4, pp.319-331, (Oct,2005).

[47] Suni PD, Percival R, Perry I eta'l, "Lasing characteristics of ytterbium, thulium, and other rare earth doped silica-based fibers", *SPIE,* 1171:244–260,(1989).

[48] D. C. Hanna, R. M. Percival, I. R. Perry, R. G. Smart, P. J. Suni, J. E. Townsend, and A. C. Tropper, "Yb-doped mono mode fiber laser: broadly tunable operation from 1.010 _m to 1.162 _m and three level operation at 974 nm," J. Mod. Opt., vol. 37, pp. 517-525, (1990).

[49] E. Snitzer, H. Po, F. Hakimi, R. Tumminelli, and B.C. McCollum, "Double-clad, offset core Nd fiber laser," in Optical Fiber Sensors,Optical Society of America, p. PD5, (1988).

[50] H. Po, E. Snitzer, L. Zenteno, F. Hakimi, N. M. Cho, and T. Haw, "Double clad high brightness nd fiber laser pumped by gaalas phased array," Digest of Optical Fiber Conf., p. PD7, (1989).

[51] M. N. Zervas, "High power ytterbium-doped fiber lasers - fundamentals and applications," Int. Journal of Mod. Phys., vol. 28, (Mar 2014).

[52] Y. Wang, W. Ke, Y. Sun, Y. Ma, T. Li, Y. Feng, and J. Wu, "Research of high brightness 1018nm ytterbium doped _ber laser," Proc. SPIE, vol. 9255, pp.92550K-92550K,(8, 2015).

[53] H. Xiao, P. Zhou, X. L. Wang, X. J. Xu, and Z. J. Liu, "High power 1018 nm Ytterbium doped fiber laser with an output power of 309 w," Laser Physics Letters, vol. 10, no. 6, p. 065102, (2013).

[54] Y. Meng, M. Salhi, A. Niang, K. Guesmi, G. Semaan, and F. Sanchez, "Mode-Locked Er: Yb-doped double-clad fiber laser with 75-nm tuning range," *Opt. Lett.* vol. 40, no.7, p. 1153, (2015).

[55] S. C. Singh, H. Zeng, C. Guo, and W. Cai, "Lasers: Fundamentals, Types, and Operations," Nanometer. Process. Charact. with Lasers, pp. 1–34, (2012).

[56] S. Ali, K. A. S. Al-Khateeb, and B. Bouzid, "A novel Erbium-Doped Fiber Laser Source (EDFL)," Proc. Int. Conf. Comput. Commun. Eng. 2008, ICCCE08 Glob. Links Hum. Dev., no. June, pp. 538–541, (2008).

[57] Zhen Li, Jun Zhou, Bing He, Xijia Gu, Yunrong Wei, Jingxing Dong, and Qihong Lou," Diode-pumped 1 018-nm ytterbium-doped double-clad fiber laser",Chinese Optics Letters,Vol.9,no.9,pp 091401,(2011).

[58] T. Sakimura et al., "1.5-μm high-gain and high-power laser amplifier using a Er,Yb:glass planar waveguide for coherent Doppler lidar," in Proc. CLEO, San Jose, p. 114 , (2012).

[59] Xiao, H., Zhou, P., Wang, X., Guo, S., & Xu, X. "Experimental Investigation on 1018-nm High-Power Ytterbium-Doped Fiber Amplifier", IEEE Photonics Technology Letters, vol.24, no.13, pp.1088–1090,(2012)

[60] Xiao, H., Zhou, P., Wang, X. L., Xu, X. J., & Liu, Z. J.,"High power 1018 nm ytterbium doped fiber laser with an output power of 309 W", Laser Physics Letters, vol.10, no.6, (2013).

[61] Sen,R.,Saha.M.,Pal.A.,Pal.M.,Leich.M.,Kobelke.J.,"High power laser fiber fabricated through vapor phase doping of Ytterbium", Laser Physics Letters, vol.11, no.8, p.085105, (2014).

[62] Wang, Y., Ke, W., Sun, Y., Ma, Y., Li, T., Feng, Y., & Wu, J." Research of high brightness 1018nm ytterbium doped fiber laser", XX International Symposium on High-Power Laser Systems and Applications, (2015).

[63] C. Ottenhues, T. Theeg, K. Hausmann, M. Wysmolek, H. Sayinc, J. Neumann, and D. Kracht, "Single-mode monolithic fiber laser with 200 W output power at a wavelength of 1018 nm," Opt. Letters, Vol.40, pp.4851–4854, (2015).

[64] Yang, H., Zhao, W., Si, J., Zhao, B., & Zhu, Y., "126 W fiber laser at 1018 nm and its application in tandem pumped fiber amplifier", Journal of Optics, vol.18,no.12,pp.125801,(2016).

[65] Glick, Y., Sintov, Y., Zuitlin, R., Pearl, S., Shamir, Y., Feldman, R., Shafir, N. "Single-mode 230 W output power 1018 nm fiber laser and ASE competition suppression", Journal of the Optical Society of America B, vol.33,no.7, p.1392,(2016)

[66] Y. Midilli, O. B. Efunbajo, B. şimşek, and B. Ortaç, "1018 nm Yb-doped high-power fiber laser pumped by broadband pump sources around 915 nm with output power above 100 W," Appl. Opt., vol. 56, no. 25, p. 7225, (2017)

[67] Kong et'al,"Efficient 240W single-mode 1018nm laser from an Ytterbium-doped 50/400μm all-solid photonic bandgap fiber", Optics Express,Vol. 26, no. 3, p.3138, (2018).

[68] Ping Yan et'al.," High-power 1018 nm ytterbium-doped fiber laser with output of 805W", Optics Letters,Vol. 42, No. 7 ,p.1193, (2017).

[69] Zou, X., Toratani, H., "Evaluation of spectroscopic properties of Yb3+-doped Glasses",Phys. Rev. B1995,vol.52,pp.15889–15897,(1995).

[70] Eger, D.; Atar, G.; Bruner, A.; Sfez, B.; Juwiler, I.; Kokki, T.; Kykkänen, P. "Spectral characterization of Yb-doped silica layers for high power laser applications", Opt.Mater, vol.33, pp.438–443, (2011).

[71] DeLoach, L.D., Payne, S.A., Chase, L.L., Smith, L.K., Kway, W.L., Krupke, W.F.,"Evaluation of absorption and emission properties of Yb3+-doped crystal for laser applications",IEEE J. Quantum Electron.vol,29,pp.1179–1191,(1993)

[72] O. G. Okhotnikov. 'Fiber Lasers", Wiley-VCH Verlag GmbH & Co. KGaA: p.294,(2012).

[73] C. Barnard, P. Myslinski, J. Chrostowski, and M. Kavehrad, "Analytical model for rare-earth-doped fiber amplifiers and lasers," IEEE Journal of Quantum Electronics, vol. 30, pp.1817–1830, (1994).

[74] Xiao, L., Yan, P., Gong, M., Wei, W., & Ou, P. "An approximate analytic solution of strongly pumped Yb-doped double-clad fiber lasers without neglecting the scattering loss", Optics Communications, vol.230,.no.(4-6), pp.401–410,(2004).

[75] R. Paschotta, J. Nilsson, A. C. Tropper, and D. C. Hanna, "Ytterbium-doped fiber amplifiers," IEEE Journal of Quantum Electronics, vol. 33, no. 7, pp. 1049–1056, (1997).

[76] J. Hecht, "Optical amplifiers," Optics & amp; Photonics News, (2002).

APPENDICES

Appendix A.1: Code for two models –Comparative code

```
%Bidirectional pumping by reference model
%For determining output power vs. input pump power
%For determining output power vs. active fiber length
%For determining combined graphs of output power
% Variables
L=1.5; %active fiber cable length
z=transpose (0:0.015:1.5); %small variation in the length
%Forward and backward pump power
Ppo=557+557*exp(z-L);%Total pump power
%pump and signal wavelengths
lp=976e-9;%pump wavelength
ls=1018e-9;%signal wavelength
WL=(960e-9:1.2e-9:1080e-9);%Wavelength range
%reflectiveness of mirror 1 and mirror 2
R1=0.995;%Highly reflective mirror
R2=0.149;%partially reflective mirror
h = 6.636e-34;%planck's constant
r=15e-6;%core radius
Na1 = 0.05; %core numerical aperture
Na2=0.46; %clad numerical aperture
%pump and signal frequencies
vp=2*pi*r*Na2/lp;%pump frequency
vs=2*pi*r*Na1/ls;%signal frequency
Aeff=pi*r^2;%effective area of the core
%absorption and emission cross section areas
dw12=0.25e-26;%das
dr12=2.4e-24;%dap
dw21=0.55e-24;%des
dr21=2.4e-24;%dep
%Transition rates
R12=(dr12*Ppo)/(Aeff*h*vp);
R21=(dr21*Ppo)/(Aeff*h*vp);
tau=0.8e-3;
% Phi for signal and pump
phis=dw12+dw21; %phi for signal sum for absorption/emission
phip=dr12+dr21; %phi for pump sum for absorption/emission
Fp = 0.015;
Fs = 1;
%pump and signal saturation powers
Pps=h*vp*Aeff/(phip*Fp*tau);%pump saturation power
Pss=h*vs*Aeff/(phis*Fs*tau);%signal saturation power
%ion level concentration
Nt=1e26;%ion density
%pump power along the fiber
PPOUT=Ppo'.*exp(-Fp*dr12*Nt*(z));
%Determining gain Gp
Gp=((Fp*phip)/(2*Fs*phis))*log(1/(R1*R2))-((((dw21*dr12)-
(dr21*dw12))/phis)*(Fp*Nt*L));
Po=((lp/ls)*((1-R2)*Pps)/(1-R2-
sqrt(R2*R1)+sqrt(R2/R1))*((Ppo/Pps)'.*(1-exp(Gp)-Gp-
(Fp*Nt*dr12*L))));
%threshold power
Pth=Pps*((Gp+(Fp*Nt*dr12*L))/1+exp(Gp));
%Determining Power out @980nm pump wavelength%
%Bidirectional pumping @980nm compared with [28]
%For determining output power vs input pump power
%For determining output power vs active cable length
```

```
%For determining output power vs varying Nt
%Mirrors %HR=99.5% OC=14.9%
% Variables
Lm=1.5;
zm=transpose(0:0.015:1.5);%small variation in the length
%Input Pump Power
Ppom=557+557*exp(zm-Lm);%Total pump power
%pump and signal wavelengths
lpm=980e-9;%pump wavelength
Na2=0.46; %clad numerical aperture
%pump and signal frequencies
vpm=2*pi*r*Na2/lpm;%pump frequency
vs=2*pi*r*Na1/ls;%signal frequency
Aeff=pi*r^2;%effective area of the core
%absorption and emission cross section areas
mdr12=2.2e-24;%dap
mdr21=1.9e-24;%dep
%Transition Rates
mR12=(mdr12*Ppom)/(Aeff*h*vpm);
mR21=(mdr21*Ppom)/(Aeff*h*vpm);
% Phi for signal and pump
phis=dw12+dw21; %phi for signal sum for absorption/emission
phipm=mdr12+mdr21; %phi for pump sum for absorption/emission
Fpm = 0.015;
%Fs = 1;
%pump and signal saturation powers
Ppsm=h*vpm*Aeff/(phipm*Fpm*tau);%pump saturation power
%Determining gain Gp
Gpm=((Fpm*phipm)/(2*Fs*phis))*log(1/(R1*R2))-((((dw21*mdr12)-
(mdr21*dw12))/phis)*(Fpm*Nt*Lm));
Gpm1=10*log(Gp);
%Determining output power at 980nm pump
Pom=((lpm/ls)*((1-R2)*Ppsm)/(1-R2-
sqrt(R2*R1)+sqrt(R2/R1))*((Ppom/Ppsm)'.*(1-exp(Gpm)-Gpm-
(Fpm*Nt*mdr12*Lm))));
Pmout=(10*log(Pom));
%Determining output power vs active fiber length@980nm
Lmf=(0:0.05:5);
zmf=transpose(0:0.05:5);%small variation in the length
Ppomf=1114;%pump power launched in the fiber
%Determining gain Gpf @980nm
Gpmf=((Fpm*phipm)/(2*Fs*phis))*log(1/(R1*R2))-((((dw21*mdr12)-
(mdr21*dw12))/phis)*(Fpm*Nt*Lmf));
%Determining power output Pof
Pomf=((lpm/ls)*((1-R2)*Ppsm)/(1-R2-
sqrt(R2*R1)+sqrt(R2/R1))*((Ppomf/Ppsm)'.*(1-exp(Gpmf)-Gpmf-
(Fpm*Nt*mdr12*Lmf))));
%Determining output power vs active fiber cable length @976nm pump
Lf=(0:0.05:5);%active cable length
zf=transpose(0:0.05:5);%small variation in the length@976nm pump
Ppof=1114;%pump power
%Determining gain Gpf @976nm
Gpf=((Fp*phip)/(2*Fs*phis))*log(1/(R1*R2))-((((dw21*dr12)-
(dr21*dw12))/phis)*(Fp*Nt*Lf));
%Determining output power
Pof=((lp/ls)*((1-R2)*Pps)/(1-R2-
sqrt(R2*R1)+sqrt(R2/R1))*((Ppof/Pps)'.*(1-exp(Gpf)-Gpf-
(Fp*Nt*dr12*Lf))));
%% Plotting Graphs
figure(1)%Input pump power vs output power
```

```
plot(Ppo,Po,Ppom,Pom),xlabel('Input Pump Power(W)'),ylabel('Output
Power (W)'),grid minor;
figure(2)%Fiber cable length vs output power
plot(zf,Pof,zmf,Pomf),xlabel('Fibre Cable Length(m)'),ylabel('Output
Power (W)'),grid minor;
figure(3)%pump power along the fiber
plot(z,PPOUT),xlabel('Fiber Cable Length
(m)'),ylabel('PPOUT(W)'),grid minor;
figure (4)%wavelength vs output power
plot(WL,Po,WL,Pom),xlabel('Wavelength (um)'),ylabel('Output Power
(W)'),grid minor;
```

End of code for comparison of models

Appendix A.2: Code for Reference model-pump power of 1154W @ 976nm wavelength

```
%Bidirectional pumping -Reference model
%For determining output power vs input pump power
%For determining output power vs active fiber length
%For determining output power vs Nt
% Variables
L=3;%active fiber cable length
z=transpose(0:0.03:3);%small variation in the length
%Forward and backward pump power
Ppo=557+557*exp(z-L);%Total pump power
%pump and signal wavelengths
lp=976e-9;%pump wavelength
ls=1018e-9;%signal wavelength
WL=(960e-9:1.2e-9:1080e-9);%Wavelength range
%reflectiveness of mirror 1 and mirror 2
R1=0.995;%Highly reflective mirror
R2=0.149;%partially reflective mirror
h = 6.636e-34;%plancks constant
r=15e-6;%core radius
Na1 = 0.05; %core numerical aperture
Na2=0.46; %clad numerical aperture
%pump and signal frequencies
vp=2*pi*r*Na2/lp;%pump frequency
vs=2*pi*r*Na1/ls;%signal frequency
Aeff=pi*r^2;%effective area of the core
%absorption and emission cross section areas
dw12=0.25e-26;%das
dr12=2.4e-24;%dap
dw21=0.55e-24;%des
dr21=2.4e-24;%dep
%Transition rates
R12=(dr12*Ppo)/(Aeff*h*vp);
R21=(dr21*Ppo)/(Aeff*h*vp);
tau=0.8e-3;
% Phi for signal and pump
phis=dw12+dw21; %phi for signal sum for absorption/emission
phip=dr12+dr21; %phi for pumpsum for absorption/emission
Fp = 0.015;
Fs = 1;
%pump and signal saturation powers
Pps=h*vp*Aeff/(phip*Fp*tau);%pump saturation power
Pss=h*vs*Aeff/(phis*Fs*tau);%signal saturation power
%ion level concentration
Nt=1e26;%ion density
%pump power along the fiber
PPOUT=Ppo'.*exp(-Fp*dr12*Nt*(z));
%Determining gain Gp
Gp=((Fp*phip)/(2*Fs*phis))*log(1/(R1*R2))-((((dw21*dr12)-
(dr21*dw12))/phis)*(Fp*Nt*L));
Po=((lp/ls)*((1-R2)*Pps)/(1-R2-
sqrt(R2*R1)+sqrt(R2/R1))*((Ppo/Pps)'.*(1-exp(Gp)-Gp-
(Fp*Nt*dr12*L))));
%threshold power
Pth=Pps*((Gp+(Fp*Nt*dr12*L))/1+exp(Gp));
%Determining output power vs active fiber cable length
Lf=(0:0.05:5);%active cable length
zf=transpose(0:0.05:5);%small variation in the length
Ppof=1114;%pump power
%Determining gain Gpf
```

```
Gpf=((Fp*phip)/(2*Fs*phis))*log(1/(R1*R2))-((((dw21*dr12)-
(dr21*dw12))/phis)*(Fp*Nt*Lf));
%Determining output power
Pof=((lp/ls)*((1-R2)*Pps)/(1-R2-
sqrt(R2*R1)+sqrt(R2/R1))*((Ppof/Pps)'.*(1-exp(Gpf)-Gpf-
(Fp*Nt*dr12*Lf))));
%% Plotting Graphs
figure(1)%Input pump power vs output power
plot(Ppo,Po),xlabel('Input Pump Power(W)'),ylabel('Output Power
(W)'),grid minor;
figure(2)%Fiber cable length vs output power
plot(zf,Pof),xlabel('Fibre Cable Length(m)'),ylabel('Output Power
(W)'),grid minor;
figure(3)%pump power along the fiber
plot(z,PPOUT),xlabel('Fiber Cable Length
(m)'),ylabel('PPOUT(W)'),grid minor;
figure (4)%wavelength vs output power
plot(WL,Po),xlabel('Wavelength (nm)'),ylabel('Output Power
(W)'),grid minor;
```

END of Code

Appendix A.3: Code for pump power of 1154W @ 980nm wavelength

```
%Bidirectional pumping at 980nm compared with Reference model
%For determining output power vs input pump power
%For determining output power vs active cable length
%For determining output power vs varying Nt
%Mirrors %HR=99.5% OC=14.9%
% Variables
L=1.5;
z=transpose(0:0.015:1.5);%small variation in the length
%Input Pump Power
Ppo=557+557*exp(z-L);%Total pump power
%pump and signal wavelengths
lp=980e-9;%pump wavelength
ls=1018e-9;%signal wavelength
WL=(960e-9:1.2e-9:1080e-9);%Wavelength range
%reflectiveness of mirror 1 and mirror 2
R1=0.995;%Highly reflective mirror%HR
R2=0.149;%partially reflective mirror%OC
h = 6.636e-34;%planck's constant
r=15e-6;%core radius
Na1 = 0.06; %core numerical aperture
Na2=0.46; %clad numerical aperture
%pump and signal frequencies
vp=2*pi*r*Na2/lp;%pump frequency
vs=2*pi*r*Na1/ls;%signal frequency
Aeff=pi*r^2;%effective area of the core
%absorption and emission cross section areas
dw12=0.25e-26;%das
dr12=2.2e-24;%dap
dw21=0.55e-24;%des
dr21=1.9e-24;%dep
%Transition Rates
R12=(dr12*Ppo)/(Aeff*h*vp);
R21=(dr21*Ppo)/(Aeff*h*vp);
tau=0.8e-3;
% Phi for signal and pump
phis=dw12+dw21; %phi for signal sum for absorption/emission
phip=dr12+dr21; %phi for pump sum for absorption/emission
Fp = 0.015;
Fs = 1;
%pump and signal saturation powers
Pps=h*vp*Aeff/(phip*Fp*tau);%pump saturation power
Pss=h*vs*Aeff/(phis*Fs*tau);%signal saturation power
%ion density to be considered%
Nt=1e26;
Nt2=1e27;
Nt3=1e25;
%pump power along the fiber
PPOUT=Ppo'.*exp(-Fp*dr12*Nt*(z));
%Determining gain Gp
Gp=((Fp*phip)/(2*Fs*phis))*log(1/(R1*R2))-((((dw21*dr12)-
(dr21*dw12))/phis)*(Fp*Nt*L));
G2=((Fp*phip)/(2*Fs*phis))*log(1/(R1*R2))-((((dw21*dr12)-
(dr21*dw12))/phis)*(Fp*Nt2*L));
G3=((Fp*phip)/(2*Fs*phis))*log(1/(R1*R2))-((((dw21*dr12)-
(dr21*dw12))/phis)*(Fp*Nt3*L));
% Gp=(Fp*phip/(2*Fs*phis))*log(1/(R1*R2))-((dw21*dw12-
dr21*dr12)/phis)*Fp*Nt*L;
Gp1=10*log(Gp);
%Determining output power at different ion concentration
```

```
Po=((lp/ls)*((1-R2)*Pps)/(1-R2-
sqrt(R2*R1)+sqrt(R2/R1))*((Ppo/Pps)'.*(1-exp(Gp)-Gp-
(Fp*Nt*dr12*L))));
Pout=(10*log(Po));
P2=((lp/ls)*((1-R2)*Pps)/(1-R2-
sqrt(R2*R1)+sqrt(R2/R1))*((Ppo/Pps)'.*(1-exp(G2)-G2-
(Fp*Nt2*dr12*L))));
P3=((lp/ls)*((1-R2)*Pps)/(1-R2-
sqrt(R2*R1)+sqrt(R2/R1))*((Ppo/Pps)'.*(1-exp(G3)-G3-
(Fp*Nt3*dr12*L))));
%threshold power
Pth=Pps*((Gp+(Fp*Nt*dr12*L))/1+exp(Gp));
%Determining output power vs active fiber length
Lf=(0:0.05:5);
zf=transpose(0:0.05:5);%small variation in the length
Ppof=1114;%pump power launched in the fiber
%Determining gain Gpf
Gpf=((Fp*phip)/(2*Fs*phis))*log(1/(R1*R2))-((((dw21*dr12)-
(dr21*dw12))/phis)*(Fp*Nt*Lf));
%Determining power output Pof
Pof=((lp/ls)*((1-R2)*Pps)/(1-R2-
sqrt(R2*R1)+sqrt(R2/R1))*((Ppof/Pps)'.*(1-exp(Gpf)-Gpf-
(Fp*Nt*dr12*Lf))));
%% Plotting Graphs
figure(1)%Input pump power vs output power @ Nt=1e26
plot(Ppo,Po),xlabel('Input Pump Power(W)'),ylabel('Output Power
(W)'),grid minor;
figure(2)%Fiber cable length vs output power
plot(zf,Pof),xlabel('Fibre Cable Length(m)'),ylabel('Output Power
(W)'),grid minor;
figure (3)%wavelength vs output power
plot(WL,Po),xlabel('Wavelength (nm)'),ylabel('Output Power
(W)'),grid minor;
figure(4)%pump power along the fiber
plot(z,PPOUT),xlabel('Fiber Cable Length
(m)'),ylabel('PPOUT(W)'),grid minor;
figure (5)%Input pump power vs output power@different Nt
plot(Ppo,Po,Ppo,P2,Ppo,P3),xlabel('Input Pump
Power(W)'),ylabel('Output Power (W)'),grid minor;
```

End of Code

Appendix A.4: Code for ion variation deploying HR=100% and OC=30%

```
%Bidirectional pumping at 980nm compared with reference model
%VARYING THE ION DENSITY %HR=100% OC=30%
% Variables
L=1.5;
z=transpose(0:0.015:1.5);%small variation in the length
%Input Pump Power
Ppo=557+557*exp(z-L);%Total pump power
%pump and signal wavelengths
lp=980e-9;%pump wavelength
ls=1018e-9;%signal wavelength
WL=(960e-9:1.2e-9:1080e-9);%Wavelength range
%reflectiveness of mirror 1 and mirror 2
R1=1;%Highly reflective mirror%HR
R2=0.3;%partially reflective mirror%OC
h = 6.636e-34;%planck's constant
r=15e-6;%core radius
Na1 = 0.06; %core numerical aperture
Na2=0.46; %clad numerical aperture
%pump and signal frequencies
vp=2*pi*r*Na2/lp;%pump frequency
vs=2*pi*r*Na1/ls;%signal frequency
Aeff=pi*r^2;%effective area of the core
%absorption and emission cross section areas
dw12=0.25e-26;%das
dr12=2.2e-24;%dap
dw21=0.55e-24;%des
dr21=1.9e-24;%dep
%Transition Rates
R12=(dr12*Ppo)/(Aeff*h*vp);
R21=(dr21*Ppo)/(Aeff*h*vp);
tau=0.8e-3;
% Phi for signal and pump
phis=dw12+dw21; %phi for signal sum for absorption/emission
phip=dr12+dr21; %phi for pump sum for absorption/emission
Fp = 0.015;
Fs = 1;
%pump and signal saturation powers
Pps=h*vp*Aeff/(phip*Fp*tau);%pump saturation power
Pss=h*vs*Aeff/(phis*Fs*tau);%signal saturation power
%ion density to be considered%
Nt=1e26;
Nt2=1e27;
Nt3=1e25;
%pump power along the fiber
PPOUT=Ppo'.*exp(-Fp*dr12*Nt*(z));
%Determining gain Gp
Gp=((Fp*phip)/(2*Fs*phis))*log(1/(R1*R2))-((((dw21*dr12)-
(dr21*dw12))/phis)*(Fp*Nt*L));
G2=((Fp*phip)/(2*Fs*phis))*log(1/(R1*R2))-((((dw21*dr12)-
(dr21*dw12))/phis)*(Fp*Nt2*L));
G3=((Fp*phip)/(2*Fs*phis))*log(1/(R1*R2))-((((dw21*dr12)-
(dr21*dw12))/phis)*(Fp*Nt3*L));
% Gp=(Fp*phip/(2*Fs*phis))*log(1/(R1*R2))-((dw21*dw12-
dr21*dr12)/phis)*Fp*Nt*L;
Gp1=10*log(Gp);
%Determining output power at different ion concentration
Po=((lp/ls)*((1-R2)*Pps)/(1-R2-
sqrt(R2*R1)+sqrt(R2/R1))*((Ppo/Pps)'.*(1-exp(Gp)-Gp-
(Fp*Nt*dr12*L))));
```

```
Pout=(10*log(Po));
P2=((lp/ls)*((1-R2)*Pps)/(1-R2-
sqrt(R2*R1)+sqrt(R2/R1))*((Ppo/Pps)'.*(1-exp(G2)-G2-
(Fp*Nt2*dr12*L))));
P3=((lp/ls)*((1-R2)*Pps)/(1-R2-
sqrt(R2*R1)+sqrt(R2/R1))*((Ppo/Pps)'.*(1-exp(G3)-G3-
(Fp*Nt3*dr12*L))));
%threshold power
Pth=Pps*((Gp+(Fp*Nt*dr12*L))/1+exp(Gp));
%% Plotting Graphs
figure(1)%Input pump power vs output power @ Nt=1e26
plot(Ppo,Po),xlabel('Input Pump Power(W)'),ylabel('Output Power
(W)'),grid minor;
figure (2)%wavelength vs output power
plot(WL,Po),xlabel('Wavelength (nm)'),ylabel('Output Power
(W)'),grid minor;
figure(3)%pump power along the fiber
plot(z,PPOUT),xlabel('Fiber Cable Length
(m)'),ylabel('PPOUT(W)'),grid minor;
figure (4)%Input pump power vs output power@different Nt
plot(Ppo,Po,Ppo,P2,Ppo,P3),xlabel('Input Pump
Power(W)'),ylabel('Output Power (W)'),grid minor;
```

End of Code

Appendix A.5: CODE for pump power of 68W @ 980nm wavelength

```
%Bidirectional pumping deploying pump power of 68watts@980nm
%For determining output power vs varying pump power
%For determining output power vs active fiber length
%For determining output power vs varying Nt
% Variables
L=0.5;%Length of the active fiber in meters
z=transpose(0:0.005:0.5);%small variation in the length
%Input Pump power in watts
Ppo=34+34*exp(z-L);%Total input pump power
Pp1=24+24*exp(z-L);%Total input pump power
Pp2=44+44*exp(z-L);%Total input pump power
Ps=1e-3;%input signal power
%pump and signal wavelengths
lp=980e-9;%pump wavelength
ls=1018e-9;%signal wavelength
WL=(960e-9:1.2e-9:1080e-9);%Wavelength range
%reflectiveness of mirror 1 and mirror 2
R1=1;%Highly reflective mirror
R2=0.30;%partially reflective mirror
%Constants
h = 6.636e-34;%planck's constant
%Core variables
r=5e-6;%core radius in micro meters
Na1 = 0.08; %core numerical aperture
Na2=0.46; %clad numerical aperture
%pump and signal frequencies
vp=2*pi*r*Na2/lp;%pump frequency
vs=2*pi*r*Na1/ls;%signal frequency
Aeff=pi*r^2;%effective area of the core
%absorption and emission cross section areas
dw12=0.25e-26;%das,signal absorption
dr12=2.2e-24;%dap,pump absorption
dw21=0.55e-24;%des,signal emission
dr21=1.9e-24;%dep,pump emission
%Transition Rates
R12=(dr12*Ppo)/(Aeff*h*vp);
R21=(dr21*Ppo)/(Aeff*h*vp);
W12=(dw12*Ps)/(Aeff*h*vs);
W21=(dw21*Ps)/(Aeff*h*vs);
tau=0.8e-3;%life time of the upper state level
%determining N1 and N2
N1=(R21+W21+(1/tau))/R12+W12+R21+W21+(1/tau);
N2=(R12+W12)/R12+W12+R21+W21+(1/tau);
% Phi for signal and pump
phis=dw12+dw21; %phi for signal sum for absorption/emission
phip=dr12+dr21; %phi for pump sum for absorption/emission
Fp = 0.0064;%pump overlap factor
Fs = 1;%signal overlap factor
%pump and signal saturation powers
Pps=h*vp*Aeff/(phip*Fp*tau);%pump saturation power
Pss=h*vs*Aeff/(phis*Fs*tau);%signal saturation power
%YB3+ ion concentration in the active fiber
Nt=1e27;%for output power Po
Nt2=1e26;% for output power P2
Nt3=1e28;%for output power P3
%pump power along the active fiber cable
PPOUT=Ppo'.*exp(-Fp*dr12*Nt*(z));
%Determining gains Gp
```

```
G2=((Fp*phip)/(2*Fs*phis))*log(1/(R1*R2))-((((dw21*dr12)-
(dr21*dw12))/phis)*(Fp*Nt2*L));
G3=((Fp*phip)/(2*Fs*phis))*log(1/(R1*R2))-((((dw21*dr12)-
(dr21*dw12))/phis)*(Fp*Nt3*L));
Gp=((Fp*phip)/(2*Fs*phis))*log(1/(R1*R2))-((((dw21*dr12)-
(dr21*dw12))/phis)*(Fp*Nt*L));
% Gain in decibels
Gp1=10*log(Gp);
%Determining output power at different ion concentration
P2=((lp/ls)*((1-R2)*Pps)/(1-R2-
sqrt(R2*R1)+sqrt(R2/R1))*((Ppo/Pps)'.*(1-exp(G2)-G2-
Fp*Nt2*dr12*L)));
P3=((lp/ls)*((1-R2)*Pps)/(1-R2-
sqrt(R2*R1)+sqrt(R2/R1))*((Ppo/Pps)'.*(1-exp(G3)-G3-
Fp*Nt3*dr12*L)));
Po=((lp/ls)*((1-R2)*Pps)/(1-R2-
sqrt(R2*R1)+sqrt(R2/R1))*((Ppo/Pps)'.*(1-exp(Gp)-Gp-
(Fp*Nt*dr12*L))));
Pout=(10*log(Po));
%Determining output power at different pump powers
Po=((lp/ls)*((1-R2)*Pps)/(1-R2-
sqrt(R2*R1)+sqrt(R2/R1))*((Ppo/Pps)'.*(1-exp(Gp)-Gp-
(Fp*Nt*dr12*L))));
P4=((lp/ls)*((1-R2)*Pps)/(1-R2-
sqrt(R2*R1)+sqrt(R2/R1))*((Pp1/Pps)'.*(1-exp(Gp)-Gp-
(Fp*Nt*dr12*L))));
P5=((lp/ls)*((1-R2)*Pps)/(1-R2-
sqrt(R2*R1)+sqrt(R2/R1))*((Pp2/Pps)'.*(1-exp(Gp)-Gp-
(Fp*Nt*dr12*L))));
%threshold power
Pth=Pps*((Gp+(Fp*Nt*dr12*L))/1+exp(Gp));
%Determining output power vs active fiber length
%For determining power vs cable length
% Variables
Lf=(0:0.05:5);
zf=transpose(0:0.05:5);%small variation in the length
%Input Pump power in watts
Ppof=68;%Total input pump power for both facets of the fiber
%Determining gain Gpf
Gpf=((Fp*phip)/(2*Fs*phis))*log(1/(R1*R2))-((((dw21*dr12)-
(dr21*dw12))/phis)*(Fp*Nt*Lf));
%Determining output power  vs active fiber length
Pof=((lp/ls)*((1-R2)*Pps)/(1-R2-
sqrt(R2*R1)+sqrt(R2/R1))*((Ppof/Pps)'.*(1-exp(Gpf)-Gpf-
(Fp*Nt*dr12*Lf))));
%% Plotting Graphs of the modeling
figure(1)%Input pump power vs output power @Nt=1e27
plot(Ppo,Po),xlabel('Input Pump Power(W)'),ylabel('Output Power
(W)'),grid minor;
figure(2)%Fiber cable length vs output power
plot(zf,Pof),xlabel('Fibre Cable Length(m)'),ylabel('Output Power
(W)'),grid minor;
figure(3)%Power output at different pump powers
plot(Ppo,Po,Pp1,P4,Pp2,P5),xlabel('Input Pump
Power(W)'),ylabel('Output Power (W)'),grid minor;
figure (4)%wavelength vs output power in watts
plot(WL,Po),xlabel('Wavelength (um)'),ylabel('Output Power
(W)'),grid minor;
figure(5)%pump power along the fiber
plot(z,PPOUT),xlabel('Fiber Cable Length
(m)'),ylabel('PPOUT(W)'),grid minor;
```

```
figure(6)%Input pump power vs output power @ different Nt
plot(Ppo,Po,Ppo,P2,Ppo,P3),xlabel('Input Pump
Power(W)'),ylabel('Output Power (W)'),grid minor;
```

End of Code

Appendix A.6: Journal Paper Publication

Paper publication in International Journal of Optoelectronic Engineering (IJOE) details:

International Journal of Optoelectronic Engineering
p-ISSN: 2167-7301 e-ISSN: 2167-731X
2021; 10 (1): 1-8
doi:10.5923/j.ijoe.20211001.01
Received: Dec. 10, 2020; Accepted: Dec. 26, 2020; Published: Jan. 15, 2021

Cite this paper: Moses Simpungwe, Charles Lubobya, Sampa Nkonde, Design of Yb^{3+} Doped Laser for Industrial Application, *International Journal of Optoelectronic Engineering*, Vol. 10 No. 1, 2021, pp. 1-8. doi: 10.5923/j.ijoe.20211001.01.